EBioMedicine 45 (2019) 139–154

Contents lists available at ScienceDirect

EBioMedicine

journal homepage: www.ebiomedicine.com

EBioMedicine
Published by THE LANCET

Aryl hydrocarbon receptor nuclear translocator-like (ARNTL/BMAL1) is associated with bevacizumab resistance in colorectal cancer *via* regulation of vascular endothelial growth factor A

Elke Burgermeister [a,*,1], Francesca Battaglin [b,c,1], Fagr Eladly [a], Wen Wu [a], Frank Herweck [a], Nadine Schulte [a], Johannes Betge [a], Nicolai Härtel [a], Jakob N. Kather [d], Cleo-Aron Weis [e], Timo Gaiser [e], Alexander Marx [e], Christel Weiss [f], Ralf Hofheinz [g], Ian S. Miller [h], Fotios Loupakis [c], Heinz-Josef Lenz [b], Annette T. Byrne [h,i,2], Matthias P. Ebert [a,2]

[a] Department of Medicine II, Medical Faculty Mannheim, University of Heidelberg, Mannheim, Germany
[b] Division of Medical Oncology, Norris Comprehensive Cancer Center, Keck School of Medicine, University of Southern California, CA, United States
[c] Unit of Medical Oncology 1, Clinical and Experimental Oncology Department, Veneto Institute of Oncology IOV - IRCCS, Padua, Italy
[d] Division of Gastroenterology, Hepatology and Hepatobiliary Oncology, University Hospital RWTH Aachen, Aachen, Germany
[e] Institute of Pathology, Medical Faculty Mannheim, University of Heidelberg, Mannheim, Germany
[f] Department of Medical Statistics, Medical Faculty Mannheim, University of Heidelberg, Mannheim, Germany
[g] Department of Medicine III, Medical Faculty Mannheim, University of Heidelberg, Mannheim, Germany
[h] Department of Physiology & Medical Physics, Royal College of Surgeons in Ireland, Dublin, Ireland
[i] UCD School of Biomolecular and Biomedical Science, Conway Institute of Biomolecular and Biomedical Research, University College Dublin, Dublin, Ireland

ARTICLE INFO

Article history:
Received 1 April 2019
Received in revised form 26 June 2019
Accepted 2 July 2019
Available online 9 July 2019

Keywords:
BMAL1
ARNTL
REVERBA
Bevacizumab
Colorectal cancer
VEGFA

ABSTRACT

Background: The identification of new biomarkers and the development of novel, targetable contexts of vulnerability are of urgent clinical need in drug-resistant metastatic colorectal cancer (mCRC). Aryl-Hydrocarbon-Receptor-Nuclear-Translocator-Like (ARNTL/BMAL1) is a circadian clock-regulated transcription factor promoting expression of genes involved in angiogenesis and tumour progression. We hypothesised that BMAL1 increases expression of the vascular endothelial growth factor A *VEGFA* gene and, thereby, confers resistance to anti-angiogenic therapy with bevacizumab (Beva), a clinically used antibody for neutralization of VEGFA.
Methods: PCR and immunohistochemistry were employed to assess BMAL1 expression in mice (C57BL/6 J $^{Apcmin/+}$; BALB/c $^{nu/nu}$ xenografts) and CRC patients under combination chemotherapy with Beva. BMAL1 single nucleotide gene polymorphisms (SNPs) were analysed by DNA-microarray in clinical samples. BMAL1 functions were studied in human CRC cell lines using colorimetric growth, DNA-binding and reporter assays.
Findings: In murine CRCs, high BMAL1 expression correlated with poor preclinical response to Beva treatment. In CRC patients' tumours ($n = 74$), high BMAL1 expression was associated with clinical non-response to combination chemotherapy with Beva ($^*p = .0061$) and reduced progression-free survival (PFS) [$^*p = .0223$, Hazard Ratio (HR) = 1.69]. BMAL1 SNPs also correlated with shorter PFS (*rs7396943, rs7938307, rs2279287*) and overall survival (OS) [*rs11022780*, $^*p = .014$, HR = 1.61]. Mechanistically, Nuclear-Receptor-Subfamily-1-Group-D-Member-1 (NR1D1/REVERBA) bound a − 672 bp Retinoic-Acid-Receptor-Related-Orphan-Receptor-Alpha-responsive-element (RORE) adjacent to a BMAL1 DNA-binding motif (*E*-box) in the *VEGFA* gene promoter, resulting in increased VEGFA synthesis and proliferation of human CRC cell lines.

Abbreviations: Ab, antibody; Apc, adenomatous polyposis coli; ARNTL (BMAL1), Aryl Hydrocarbon Receptor Nuclear Translocator-Like; B2M/B2m, beta-2-microglobulin; Avastin®, Beva human bevacizumab; B20, mBeva murine bevacizumab; CAV1, caveolin-1; CMS, consensus molecular subtype; CRC, colorectal cancer; DCR, disease control rate (PR + SD); DFS, disease-free survival; *E*-box, BMAL1/MYC-responsive (DNA) element; ECOG, Eastern Cooperative Oncology Group; FFPE, formalin-fixed paraffin-embedded; G grade, (tumour); GEMM, genetically engineered mouse model; HE, haematoxylin & eosin; HIF1A, Hypoxia-Inducible Factor-1 Alpha; HR, hazard ratio; IHC, immunohistochemistry; KO, knock-out; MVD, microvessel density; N, nodal status (tumour); NC, normal colon (tissue); NR, non-responder; NR1D1 (REVERBA), Nuclear Receptor Subfamily 1 Group D Member 1; NT, non-tumour (normal); OS, overall survival; PCA, principal component analysis; PD, progressive disease; PFS, progression-free survival; PR, partial response; R, responder; RECIST, Response Evaluation Criteria In Solid Tumours; RORA, Retinoic Acid Receptor-Related Orphan Receptor Alpha; RORE, ROR responsive (DNA) element; SD, stable disease; SI, small intestine; SNP, single nucleotide polymorphism; T, size (tumour); TMA, tissue microarray; TU, tumour; UICC, Union internationale contre le cancer (tumour stage); VEGF(R), vascular endothelial growth factor (receptor).

* Corresponding author at: Dept. of Medicine II, Universitätsklinikum Mannheim, Medical Faculty Mannheim, University Heidelberg, Theodor-Kutzer Ufer 1-3, D-68167 Mannheim, Germany.
E-mail address: elke.burgermeister@medma.uni-heidelberg.de (E. Burgermeister).
[1] Equal contribution.
[2] Joint senior authors.

https://doi.org/10.1016/j.ebiom.2019.07.004

Interpretation: BMAL1 was associated with Beva resistance in CRC. Inhibition of REVERBA-BMAL1 signalling may prevent resistance to anti-angiogenic therapy.
Fund: This work was in part supported by the European Commission Seventh Framework Programme (Contract No. 278981 [ANGIOPREDICT]).

1. Introduction

Colorectal cancer (CRC) is the third most commonly diagnosed malignancy in both men and women and represents a major component of worldwide cancer mortality and morbidity [1]. Current treatment for metastatic CRC (mCRC) includes 5-fluoruracil-based standard of care chemotherapy (*e.g.* FOLFOX, FOLFIRI) combined with bevacizumab (Beva). Beva is a human monoclonal antibody (Ab) that prevents binding of vascular endothelial growth factor A (VEGFA) to its receptors [1], thus inhibiting angiogenesis. Nevertheless, only a subset of patients responds, and resistance to anti-angiogenic therapy may be intrinsic or adaptive in nature [2]. The underlying molecular mechanisms have yet to be fully revealed. Elucidation of the biology underpinning treatment failure, and the identification of novel predictive markers to identify CRC patients who will benefit from Beva therapy continues to hold clinical relevance [2].

To this end, we studied transcription factors of the circadian clock machinery which had been previously reported to regulate *VEGFA* gene expression [3–6] and, thus, may represent suitable candidates for mediating Beva resistance. Synchronised by the solar input to the suprachiasmatic nucleus of the hypothalamus and other brain regions, the "central clock" orchestrates complex signalling networks termed "peripheral clocks" in tissues and organs on an approximate 24 h day/night cycle [7,8]. At the cellular level, these circuits are driven by the master activator basic helix-loop-helix transcription factor "Aryl Hydrocarbon Receptor Nuclear Translocator-Like" (ARNTL/BMAL1, herewith termed BMAL1) and its heterodimer partner "Circadian Locomotor Output Cycles protein Kaput" (CLOCK) [9]. This complex binds to DNA-motifs (*E*-boxes) in regulatory regions of genes encoding for activating (*e.g. Retinoic Acid Receptor-Related Orphan Receptor Alpha*, *RORA*) and repressive (*e.g. Nuclear Receptor Subfamily 1 Group D Member 1*, *NR1D1*/*REVERBA; PER1/2*, *CRY1/2*) transcription factors inducing negative transcriptional/translational feed-back mechanisms which ultimately generate diurnal oscillations of output genes [7,8]. RORA binds oxysterols, REVERBA nitric oxide, carbon monoxide or Fe(II/III)-heme derived from degraded red blood cells. Both receptors compete for the same site on the DNA, termed ROR responsive element (RORE) [8] and, thereby, regulate target genes, such as BMAL1 and *Hypoxia-Inducible Factor-1-Alpha* (*HIF1A*), in a reciprocal mode of fashion. Overall, these properties position circadian clock transcription factors as important sensors of the tissue's redox and oxygenation status [7,8]. Accordingly, they regulate down-stream genes responsible for the maintenance of cardio-vascular homeostasis, body temperature, metabolism, immune defence and developmental or regenerative processes such vasculo- and angiogenesis.

The pivotal role of BMAL1 in orchestrating this hierarchy of regulatory circuits and its cooperation with tissue-specific non-circadian transcription factors [9] provided the rationale to explore its role in resistance to anti-angiogenic therapy: BMAL1 is implicated in several aspects of vessel (dys)function, *i.e.* coverage of endothelia by pericytes, coagulation / thrombosis, vascular tone / hypertension and atherosclerosis [7,8]. Specifically, BMAL1 is a stimulator of VEGFA production having previously been shown to up-regulate *Vegfa* promoter activity in mouse xenografts [3]. Conversely, *Bmal1* silencing lowered *Vegfa* mRNA in genetically engineered mouse models (GEMMs) [4,5] and impaired vessel growth in zebrafish [6].

In contrast to the normal body physiology, aberrant expression or arrhythmic activities endow BMAL1 (and other circadian transcription factors) with more specialised functions in disease conditions [7,8]. Clock disruptions, by sleep deprival (*e.g.* jet lag, shift work, neuropsychiatric disorders) or gene mutations, are associated with metabolic or inflammatory disturbances and presumably with an enhanced risk for cardiovascular diseases and cancer [10]. Oncogenes (*e.g.* MYC, RAS) or loss of tumour suppressors (*e.g.* PTEN) destroy circadian rhythms in cancer cells. For example, mutant KRAS abrogates oscillation cycles of BMAL1 [11], and MYC out-competes BMAL1 at shared *E*-boxes [12] on target genes. In murine CRC [13] and liver metastases [14], the amplitude and phase of circadian rhythmicity in BMAL1 expression were attenuated, delayed or fully abolished. Thus, a deregulated clock is implicated as a hallmark of cancer [7,8].

In tumour cells, BMAL1 regulates expression of genes/proteins [9] involved in cell proliferation, stemness, senescence or cell survival (*P21*, *CDC25A*), endoplasmic reticulum-mediated stress resilience (eIF2α), evasion of apoptosis, *e.g. via* DNA-damage repair pathways (p53, ATM), cell migration (*ROCK2*, *MTA1*), hypoxia (*HIF1A*) or systemic immune responses (*CXCL2*), supporting a role for BMAL1 as a potential oncogene contributing to chemotherapy resistance or metastasis [7,8]. In patients, high BMAL1 expression has been associated with advanced CRC as well as other cancers [15]. Based on this evidence, we hypothesised that BMAL1 could have a predictive and/or mechanistic involvement in Beva resistance and sought to investigate its role in CRC.

Research in context

Evidence before this study

Transcription factors of the circadian clock (such as BMAL1) determine resistance to radiation and chemotherapy in cancer patients. However, their role regarding the efficacy of current targeted therapies such as antibodies against growth factors (like VEGFA) or their receptors remains elusive.

Added value of this study

We identified BMAL1 as a potential marker and functional player in resistance to clinically-in-use VEGFA-neutralizing antibody (bevacizumab) in preclinical, clinical and cellular mechanistic studies of colorectal cancer.

Implications of all the available evidence

Failure to respond to bevacizumab correlated with high expression of BMAL1, a transcription factor which drives persistent synthesis of VEGFA in and secretion from tumour cells. In translational studies, BMAL1 shall be further developped as a predictive biomarker detecting and/or as a druggable target preventing resistance to anti-angiogenic therapy in colorectal cancer patients.

2. Materials and methods

2.1. Reagents

Chemicals were from Merck (Darmstadt) or Sigma (Taufkirchen), Germany. mBeva (mu_chimeric_B20–4.1) was provided on contract by Roche Diagnostics, Penzberg, Germany (MTA#10082012). Beva (Avastin®) was purchased from the hospital pharmacy [16]. Abs for Western blots were REVERBA (#PA-29865, Thermo Fisher Scientific (FS), Darmstadt, Germany), BMAL1 (sc-48790) and HSP90 (sc-7947) (all from Santa Cruz Biotech., CA). Abs for immunohistochemistry (IHC) were Ki67 (#550609, BD Bioscience, Heidelberg, Germany), CD31 (#Clone SZ31, Dianova, Hamburg, Germany), BMAL1 (#NBP2–02544, for human, Novus Biologicals, Littleton, CO), BMAL1 (#NB100–2288, for mouse, Novus). siRNA oligonucleotides were from Dharmacon (Thermo FS). Human REVERBA (67 kDa, NM_021724, MHS1010–9205700) and BMAL1 (69 kDa, NM_001178.5, MHS6278–202757260) were obtained as full-length cDNA clones in pCMV SPORT6 (Thermo FS). Proximal promoter regions of the human *VEGFA* (−2 kb/+1) gene were PCR amplified and inserted into pGL3-luc (Promega, Madison, WI). Oligonucleotides are listed in Supplementary Table 1.

2.2. Patient studies

Tissue microarrays (TMAs) of drug-naïve CRC patients ($n = 48$) were purchased from US Biomax (Co483, Rockville, MD). Therapy studies were conducted in accordance with ethical guidelines (Declaration of Helsinki) and approved by the local ethics committees for each participating site. All patients provided written informed consent for the analysis of molecular correlates. Treatment of CRC patients, for the first cohort retrospectively examined ($n = 77$), was performed as described [17,18]. Surgical specimens [Union internationale contre le cancer (UICC) stage II-IV] were collected prior to any therapy and subjected to histological evaluation according to the Vienna classification [19]. Patients then underwent first-line single or multiple chemotherapy regimens (based on FOLFOX, FOLFIRI) in combination with Beva. Patients were stratified into responders (R) and non-responders (NR) according to progression-free survival (PFS) with a cut-off of 300 days (10 months). PFS was defined as time from start of chemotherapy until the first observed progression. Subgroups were classified by clinical performance following Beva treatment based on restaging examinations according to Response Evaluation Criteria In Solid Tumours (RECIST) [18,20]: Cases were stratified by complete response (CR), partial response (PR), stable disease (SD), progressive disease (PD) or death. Patients who were staged as CR, PR or SD were attributed to the disease control rate (DCR) group (R) *vs.* PD (NR). In a separate cohort, the impact on the clinical outcome of four single nucleotide polymorphisms (SNPs) in the BMAL1 (*ARNTL*) gene (Supplementary Table 2) was evaluated in mCRC patients ($n = 215$) treated with first-line FOLFIRI plus Beva in the randomised phase III TRIBE trial [21,22]. Primary endpoint was PFS, and secondary endpoints were overall survival (OS) and tumour response. PFS was defined as time from randomization until disease progression, death or until last follow up in patients who were alive and remained free of disease progression. OS was defined as time from randomization until death. In both cohorts, patients who had no event observed were censored at the last date of follow up.

2.3. Single nucleotide polymorphism (SNP)

Molecular analyses were performed at the USC / Norris Comprehensive Cancer Center in Los Angeles. The study was conducted adhering to the reporting recommendations for tumour marker prognostic studies [23]. Potentially functional SNPs of interest within the BMAL1 (*ARNTL*) gene in the randomised phase III TRIBE trial [21,22] were identified according to the following criteria: minor allele frequency > 10% in Caucasians; potential to change gene function in a relevant matter according to public databases (National Institute of Environmental Health Science SNP Function Prediction, snpinfo.niehs.nih.gov, Queen's University F-SNP, compbio.cs.queensu.ca, NCBI-Pubmed and dbSNP, www.ncbi.nlm.nih.gov as well as Genecards, genecards.org) or tagging SNPs. Linkage disequilibrium among selected SNPs was evaluated by means of SNAP search service (http://archive.broadinstitute.org/mpg/snap/). Genomic DNA from peripheral blood samples was extracted using the QIAmp DNA Mini Kit (Qiagen, Valencia, CA) according to the manufacturer's protocol and genotyped through the OncoArray™ platform, a custom array manufactured by Illumina (San Diego, CA), including approximately 530 K SNP markers [24]. Four SNPs in BMAL1 were analysed: *rs11022780, rs7396943, rs7938307* and *rs2279287* (Supplementary Table 2).

2.4. Animal studies

Animal studies conducted in Germany (35–9185.82/G-176/12;81/G-146/15;81G-188/18) were approved by the government of Baden-Württemberg (Karlsruhe, Germany) and the local institutional board of Heidelberg University. The facilities guaranteed 12 h light on-off cycles at constant room temperature. Animals were injected and sacrificed between 10 a.m. and 2 p.m. to avoid sampling errors due to circadian phases. Animals from inbred strain [25] *Apc* $^{min/+}$ (C57BL/6 J; Charles River Labs., Wilmington, MA) *Cav1* $^{+/-}$ (Cav1tm1Mls/J; #004585; Jackson Labs., Bar Harbor, Maine) were randomised (at an age of 4–5 month) according to sex and body weight. Tumour-bearing animals were identified by rectal bleeding and *Apc* $^{min/+}$ genotype. Mice ($n = 11$) were injected (i.p., 10 mg/kg, once a week) with mBeva (Roche Diagnostics GmbH, Penzberg) for 4 weeks. Controls comprised tumour-bearing littermates of matched generations ($n = 42$). Recombinant murine Ab was provided by Roche under material transfer agreement. mBeva (mu_chimeric_B20–4.1 [26]; G6–31 equivalent [27]; [3.08 mg/ml]) neutralises human and mouse VEGFA and has a murine invariant backbone of the Ab chains for applications in immunocompetent mice. Xenograft studies conformed to the 2010/63/EU guidelines and were approved by the Dept. of Health and Children, Dublin, Ireland (B100/3654) and University College Dublin Animal Research Ethics Committee (P12–27). Briefly, BALB/c $^{nu/nu}$ mice ($n = 48$, Charles River Labs., UK) were subcutaneously implanted with 2×10^6 HCT116 cells in the right flank as previously described [28], and tumours were grown until they reached 200 mm^3. Subsequently, animals were randomised into four cohorts ($n = 12$ per group) and treated with either vehicle [5% (*w*/*v*) glucose and PBS] or clinically relevant doses of Beva [10 mg/kg, i.p. once a week] and FOLFOX [Folinic acid: 13.4 mg/kg, 5-FU: 40 mg/kg, Oxaliplatin: 2.4 mg/kg.; i.p. once a week 24 h before Beva] either alone or in combination for 4 weeks.

2.5. Cell culture

Simian Virus 40 (SV40) large T-antigen transformed human embryonic kidney (HEK293T) and human colon adenocarcinoma (SW480, HCT116) cell lines (all purchased from the American Type Culture Collection, Rockville, MD) were cultivated in Dulbecco's Modified Eagle's Medium (DMEM) (#41965) supplemented with 10% (*v*/*v*) fetal calf serum (#SV30160), 20 mM glutamine and penicillin / streptomycin (1000 U/ml; all from Thermo FS), herewith termed "complete" medium, as recommended by the distributors. CRC cell lines were chosen based on their mutational status for the *KRAS* gene and Wnt-pathway components, the major oncogenic drivers of the largest consensus molecular subgroups (CMS2/3) of human CRC [29]. Cell lines were routinely tested (every 3 months) using PlasmoTest™ (#17C01-MM, Mycoplasma Detection Kit, InVivoGen, Toulouse, France). Cell cultivation did not exceed 25 consecutive passages after thawing from liquid N_2. Transfection procedures were done as described by the manufacturer of TurboFect® reagent (Thermo FS). Colorimetric cell viability assay based on

3-(4,5-dimethylthiazol-2-yl)-2,5-diphenyltetrazolium bromide (MTT) was conducted according to the manufacturer's protocol (Roche Diagnostics GmbH, Mannheim, Germany). Enzyme-linked immunosorbent assay (ELISA) was done as recommended by the distributor (DVE00, R&D Systems, Minneapolis, MN) measuring VEGFA in supernatants of monolayer cell cultures. Conditioned medium (CM) was prepared by growing cells for 72 h to subconfluency in 6-cm dishes using complete DMEM, followed by collection of supernatants and storage at −80 °C. Starvation medium (SM) was composed of basal DMEM without any supplements. Clinically relevant mBeva (1–10 μg/ml) [30] and non-toxic hemin (≤30 μM) [31] concentrations were applied for *in vitro* assays.

2.6. Western blotting

The methods including preparation of cell and tissue protein lysates were done as described previously [32].

2.7. Reverse transcription PCR (RT-PCR) and quantitative PCR (qPCR)

Methods were performed on total RNA as published [25]. PCR primers are listed in Supplementary Table 1.

2.8. Electrophoretic mobility shift assay (EMSA)

Biotin-labelled oligonucleotides (Supplementary Table 1) were annealed and served as a binding probe for nuclear extracts as described before [33] and following the guidelines of the manufacturer (LightShift Chemiluminescent EMSA Kit, Thermo FS).

2.9. Chromatin-immunoprecipitation (ChIP)

ChIP was conducted as published previously [34] followed by genomic qPCR using primers as indicated in Supplementary Table 1.

2.10. Immunohistochemistry (IHC)

Ab and haematoxylin & eosin (HE) stainings were performed on formalin-fixed paraffin-embedded (FFPE) samples as described [35]. IHC was done manually on murine samples or using Dako Autostainer Plus (Agilent, Santa Clara, CA) on human specimens. Abs were diluted as recommended by the manufacturers, and 3,3′-diamino benzidine (DAB, brown colour) was employed for detection (Vectorlabs, Burlingame, CA). Automatised calculation of CD31+ microvessel density (MVD) and vessel size followed an established protocol [36]. Staining frequency and intensity in epithelial [(tumour (TU); non-tumour/normal (NT)] and stroma (lamina propria) cells were analysed observer-blinded [35]. Scores were: 0+ = negative (0–25%), 1+ = weak (25–50%), 2+ = moderate (50–75%), 3+ = strong (75–100% positive nuclei compared to total nuclei per field). Images from bright field microscopy (DM BE Quantimet 600 HR, Camera: DC500, Software: IM50, Leica Microsystems, Wetzlar, Germany) were manually quantified using the software Image J (https://imagej.nih.gov/ij/) ($n > 50$ nuclei per field, $n = 5$ fields per image).

2.11. cDNAmicroarray

As published before [25], cRNAs from CRC and adjacent normal colon tissue of *Apc* $^{min/+}$ *Cav1* $^{+/-}$ mice were hybridised to GeneChip® Mouse Exon 1.0 ST arrays (Affymetrix, Wycombe, UK), followed by Gene Set Enrichment Analysis (GSEA). CEL files were submitted to the NCBI GEO data set repository with the accession number GSE124838 and ID 200124838 under the following link: https://www.ncbi.nlm.nih.gov/geo/query/ acc.cgi?acc = GSE124838.

2.12. Software and statistics

Results are means ± S.E. from at least 3 subjects or mice per genotype and treatment group or independent cell passages. Data were normalised to house keeper genes or proteins as indicated in legends to figures and calculated as % or fold *vs.* control. Matched tumour (TU) and normal/non-tumour (NT) intestinal tissues from the same patient or mouse were assessed. Graphpad Prism (version 4.0; GraphPad Software, San Diego, CA) and SAS (version 9.3; SAS Institute, Cary, NC) were used to analyse the data. All tests were two-sided. *P*-values $^*p <$ .05 were considered significant. Transcription factor binding sites were identified with AliBaba2.1 (gene-regulation.com/pub/programs/alibaba2/) based on TRANSFAC 4.0.

For SNP-analysis, Kaplan-Meier curves and log-rank test were used in univariate analysis; events/total, Hazard Ratio (HR), median and Wald P-value were based on multivariable Cox proportional hazards regression models adjusting for patient characteristics including gender, age, Eastern Cooperative Oncology Group (ECOG) performance status, primary tumour site, primary tumour resected, liver limited disease, adjuvant chemotherapy, *BRAF* status, *RAS* status, and top three principle components from the principal component analysis (PCA) for European ancestry SNPs [23,24]. The associations between SNPs and tumour response were evaluated using chi-square test. Exploratory subgroup analyses by gender, primary tumour location, and *RAS* mutational status were also performed. Interaction test for SNPs and gender, tumour location and *RAS* status was conducted using the same multivariable Cox proportional hazard models. All *P*-values were from two-sided Wald tests at a 0.05 significance level. All tests were calculated by using the SAS statistical package version 9.4.

3. Results

3.1. mBeva reduces CRC growth in GEMMs

To explore mBeva efficacy *in vivo*, we employed a genetically engineered mouse model (GEMM) that develops macroscopic vascularised CRC driven by co-deficiency of adenomatous polyposis coli (*Apc*) and caveolin-1 (*Cav1*) as previously described [25]. Gene set enrichment analysis of cDNA microarrays (GSE124838) revealed a pro-invasive signature in CRCs from *Apc* $^{min/+}$ *Cav1* $^{-/+}$ mice [25]. Likewise, iron-regulated genes were up-regulated in tumour (TU) *vs.* non-tumour/normal (NT) colon tissue by >2 to 60-fold (Supplementary Table 3, Supplementary Fig. 1). Minor changes were recorded for clock-related genes (*e.g. Clock, Reverbb e.a.)*, prompting us to assess whether those transcription factors play a role in CRC *in vivo*.

To this end, tumour-bearing *Apc* $^{min/+}$ *Cav1* $^{-/+}$ mice ($n = 11$) were treated (i.p.; 10 mg/kg once a week) with mBeva for 4 weeks. The control cohort comprised tumour-bearing littermates of matched generations ($n = 42$). Mice were sacrificed, and serum and organs collected for cryopreservation or formalin-fixed paraffin embedding (FFPE). Macroscopic (Fig. 1a) and microscopic (Fig. 1b) histopathological analyses of murine tissues were performed to determine the response to mBeva treatment (Supplementary Tables 4–5). mBeva decreased incidence and multiplicity of CRC: 30 of 42 (71.4%) controls bore colon tumours *vs.* 4 of 11 (36.4%) treated mice ($^*p = .0411$, Fisher Exact test) (Fig. 1c), and 11 of 42 (26.2%) controls had >1 colon tumour *vs.* 0 of 11 (0%) treated animals (Cochrane Armitage trend test, $^*p = .0157$) (Fig. 1d). In sum, 27 of 42 (64.3%) controls had high-grade tumours *vs.* 1 of 11 (9.1%) treated mice ($^*p = .0015$, Fisher Exact test) (Fig. 1e), and 21 of 42 (50%) tumours displayed dilated glands ("cysts"), ulcerations with hemorrhage and other signs for cell death compared with 1 of 11 (9.1%) under therapy ($^*p = .0172$, Fisher Exact test) (Fig. 1f).

In addition, tumour size was reduced from [9.7 ± 12 mm^2] in controls to [5.8 ± 2.8 mm^2] following treatment (Supplementary Tables 4–5), and the percentage of stromal cells within tumours was higher in treated [60.0 ± 14.1 $n = 4$] than in control mice [30.8 ±

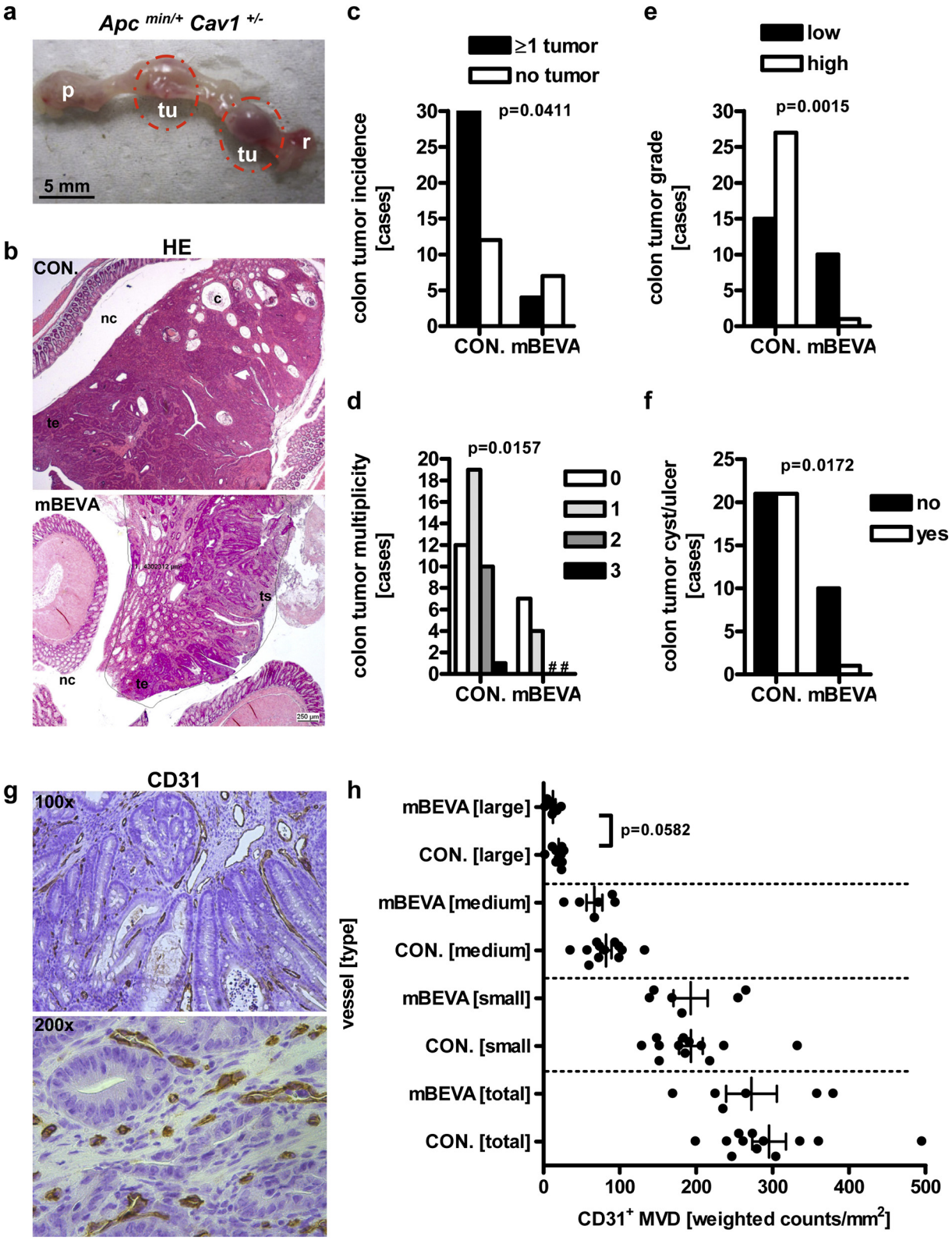

Fig. 1. mBeva inhibits CRC growth in GEMMs. (a) Macroscopic representative image of (2 adjacent) vascularised distal CRCs in a resected colon from *Apc* $^{min/+}$ *Cav1* $^{-/+}$ mice. Original magnification 10×. tu = tumour, p = proximal, r = rectum. Scale bar = 5 mm. (b) Microscopic representative images of HE-stained FFPE colon tissue sections from control and mBeva-treated *Apc* $^{min/+}$ *Cav1* $^{-/+}$ mice. nc = normal colon, te = tumour epithelial region, ts = tumour stroma region, c = cyst/dilated gland. Original magnification 50×. Scale bar = 250 µm. (c) mBeva reduces incidence of CRCs. *Apc* $^{min/+}$ *Cav1* $^{-/+}$ mice were treated with mBeva (i.p., 10 mg/kg, once per week) for 4 weeks. Data are absolute case numbers (mice with or without tumours) (*$p = .0411$ mBeva *vs.* control, Fisher Exact test). (d) mBeva reduces multiplicity of CRCs. Data are presented as in panel c (number of tumours per mouse) (*$p = .0157$ mBeva *vs.* control, Cochran Armitage trend test). # = no cases recorded. (e) mBeva reduces colon tumour grade (G), *i.e.* improves histomorphology from "high-grade/dedifferentiated" to "low-grade/well-differentiated". Data are absolute numbers [cases] from $n \geq 11$ animals per group (*$p = .0015$ mBeva *vs.* control, Fisher Exact test). (f) mBeva reduces colon tumour ulcers/cysts. Data are absolute numbers [cases] from $n \geq 11$ animals per group (*$p = .0172$ mBeva *vs.* control, Fisher Exact test). (g–h) mBeva has no effect on microvessel density (MVD). Immunohistochemistry (IHC) detecting CD31 in *Apc* $^{min/+}$ *Cav1* $^{-/+}$ CRC tissue sections: (g) Representative images. Original magnifications 100×, 200×. (h) Quantitative analysis of MVD by vessel size. Data are means (weighted counts of CD31+ vessels per mm^2) ± S.E. from $n \geq 6$ animals per group (large vessels: $p = .0582$ mBeva *vs.* control; *t*-test procedure). Detailed statistics for all preclinical parameters is presented in Supplementary Tables 4–6.

15.8 $n = 25$] (*$p = .0123$, Wilcoxon two-sample test). Treated animals had less sub-epithelial lymphoid follicles (excluding Peyer's Patches) [0.3 ± 0.6 $n = 11$] in the intestine than controls [2.7 ± 3.5 $n = 34$] (*$p = .0017$, Wilcoxon two-sample test) and fewer adenomas in the small intestine (SI) (Supplementary Fig. 2).

To assess the ability of mBeva to attenuate neoangiogenesis, *i.e.* tumour vessel growth, immunohistochemistry (IHC) was conducted on FFPE-tissue sections of *Apc* $^{min/+}$ CRCs. We employed CD31 (Platelet/Endothelial Cell Adhesion Molecule-1, PECAM1) as a surrogate marker for *in situ* detection of microvessel density (MVD) [37]. However, morphometric quantification of MVD based on CD31+ staining positivity failed to uncover differences between mBeva-treated and untreated tumour-bearing mice (Fig. 1g-h). There was a trend towards reduction of large vessels following treatment (counts per mm^2: 12.4 ± 7.9 mBeva $n = 6$ *vs.* 19.8 ± 6.9 control $n = 12$, $p = .0582$, *t*-test procedure) (Supplementary Table 6). Thus, neutralization of VEGFA *in vivo* prevented CRC growth in mice without a major impact on neoangiogenesis.

3.2. BMAL1 is associated with murine CRCs that were resistant to mBeva therapy

To gain further understanding as to why mBeva fails to reduce MVD *in vivo*, RT-qPCRs on total RNA extracted from intestinal organs were performed. We focussed on BMAL1 based on its recognised role in cancer therapy resistance [7,8]. *Arntl* (herewith termed *Bmal1)* mRNA was up-regulated in small intestinal tissue from untreated *Apc* $^{min/+}$ (MIN) compared with untreated wildtype (WT) animals (MIN 2.0 ± 0.5 *vs.* WT 0.7 ± 0.1-fold, *$p = .0043$, Mann Whitney test, n = 6 per group) (Fig. 2a). Similar results were obtained for *Vegfa*, and a trend was stated for *Cd31*. Notably, mBeva did not attenuate *Bmal1* mRNA ($p = .0576$, Kruskal Wallis test, $n = 9$ per group) in colon tissue from mBeva-treated *vs.* untreated tumour-bearing *Apc* $^{min/+}$ mice (Fig. 2b). Likewise, *Vegfa* and *Cd31* remained elevated. These findings indicated that VEGFA neutralization despite attenuation of tumour growth fails to reduce vessel formation *in vivo*, presumably by up-regulation of alternate pathways, such as BMAL1.

To measure BMAL1 protein, IHC was performed on CRC tissue from treated tumour-bearing *Apc* $^{min/+}$ mice (Fig. 2c). Responder (R) *vs.* non-responder (NR) mice were defined by 2D tumour areas (NR > 6 mm^2 > R) and the proliferation marker Ki67. Notably, high BMAL1 staining was associated with preclinical non-response of individual mice to mBeva. Accordingly, BMAL1 protein expression was decreased in CRCs of R compared with NR animals ($p = .0821$ Fisher Exact test; *$p = .0447$ *t*-test), and R mice were characterised by smaller tumour size and lower Ki67+ ($p = .0695$ Fisher Exact test; *$p = .0170$ t-test) proliferation index ($n = 4$ per group, R *vs.* NR). Collectively, these data proposed that failure of mice to respond to mBeva correlates with high BMAL1 expression.

3.3. Beva treatment correlates with BMAL1 protein expression in mouse CRC xenografts

To interrogate the association of BMAL1 expression with human VEGFA Ab (Beva) treatment in an independent animal model, CRC tissues from HCT116 xenografts were analysed. Tumour-bearing mice ($n = 12$ per group) were subjected to a 4-weeks treatment (i.p.) with vehicle (5% glucose *w/v*), Beva (10 mg/kg), FOLFOX (40 mg/kg 5-FU; 3.4 mg/kg oxaliplatin; 13.4 mg/kg folinic acid) or FOLFOX followed by Beva 24 h later (as detailed in *Materials & Methods*). After 4 weeks, mice treated with FOLFOX in combination with Beva had tumours significantly smaller (*$p < .001$ FOLFOX+Beva *vs.* vehicle control, t-test) than mice with tumours treated with either monotherapy arms or vehicle (Fig. 2d). At the end of 4 weeks, mice were euthanised, and tumours were harvested. FFPE-tissue sections were stained with BMAL1 Ab by IHC (Fig. 2e). Histopathologic evaluation of positivity scores demonstrated that Beva not only failed to lower BMAL1 protein in xenografts but rather increased its expression (75 ± 5% Beva *vs.* 40 ± 7% vehicle control, $n = 4$ per group,*$p = .0286$, Mann Whitney test). BMAL1 protein was also detected in murine and patient (pos. control) tissue lysates subjected to Western blotting (Fig. 2f). Thus, resistance to mBeva was associated with high BMAL1 expression, both in GEMM and xenograft CRC mouse models.

3.4. Clinical non-response to Beva correlates with BMAL1 protein expression in CRC

To determine BMAL1 protein expression in CRC patients, IHC studies were first performed on tissue microarrays (TMAs) of tumour (TU, $n = 40$) and non-tumour/normal colon (NT, $n = 8$) specimens from drug-naïve cases. BMAL1 staining (Supplementary Fig. 3) was reduced (by ~50% TU *vs.* NT) in tumour compared with normal colon tissue in both epithelial and stromal (lamina propria) cells. BMAL1 positivity decreased with increasing tumour aggressiveness [19], such as cellular dedifferentiation (grade, G), growth into submucosal layers (size, T) and invasion of local lymph nodes (nodal status, N) (*$p < .05$ *vs.* NT, Kruskal Wallis test). Still, a major proportion of patients (33 of 40 / 83%) retained BMAL1 staining in tumour cells, which justified subsequent studies regarding its possible connection to therapy response.

Therefore, to assess whether BMAL1 could serve as a marker of Beva resistance in humans, a retrospective series of CRC tissue specimens (TU, $n = 77$) was analysed by IHC (Supplementary Tables 7–10) [17,18]. There was a significant association between low BMAL1 staining (scores 0/1) in tumour cells and stable disease (SD) in patients undergoing Beva therapy (Cochrane Armitage trend test *$p = .0061$; Fisher Exact test *$p = .0130$; $n = 44$) (Fig. 3a). Accordingly, high BMAL1 staining (scores 2/3) in the tumour correlated with progressive disease (PD) (Fisher Exact test $p = .0987$; n = 44) (Fig. 3b). Consistently, patients who had high BMAL1 staining in their tumour tissue were less likely to belong to the disease control rate group (DCR: PR/SD) responding to Beva (R *vs.* NR, Cochrane Armitage trend test $p = .0921$; $n = 63$) (Fig. 3c).

Analysis of progression-free survival (PFS) data demonstrated that high BMAL1 protein expression in tumour cells correlated with poor clinical outcome [R (PR/SD) *vs.* NR (PD/Death); scores 0–2 *vs.* 3: Fisher Exact test *$p = .0413$; n = 77] (Fig. 3d). Data for individual patient cases from restaging examinations according to Response Evaluation Criteria In Solid Tumours (RECIST) [20] are shown in Supplementary Fig. 4. High BMAL1 positivity in tumour tissue was also associated with the likelihood to show a progress (PD) in the first restaging according to RECIST (Supplementary Fig. 5).

Overall, high BMAL1 protein expression in tumours was associated with reduced PFS (Fig. 3e). Kaplan-Meier patient survival curves by PFS in months ($n = 74$ cases) were plotted according to the first observed progress (PD) according to RECIST *vs.* BMAL1 staining scores: [0–2 *vs.* 3: $p = .1667$ log rank test, HR = 1.601 (95% CI 0.79–3.84); *$p = .0399$ Wilcoxon test]. Additional pair-wise comparisons are presented in (Supplementary Fig. 6): [2 *vs.* 3: $p = .1617$ log rank test, HR = 1.687 (95% CI 0.79–4.18); *$p = .0223$ Wilcoxon test]. Collectively, these results indicate that a high BMAL1 expression in tumours correlates with a poor clinical outcome following Beva treatment.

Further analysis of an independent cohort of CRC patients using cBioPortal of Cancer Genomics™ [38] [Colorectal Adenocarcinoma, TCGA, Provisional, $n = 633$] (Supplementary Table 11, Supplementary Fig. 7) underscored that alterations in the BMAL1 (*ARNLT*) gene, mainly amplifications, mutations and changes in mRNA transcription, confer poor prognosis. However, due to limited case numbers, significance was not reached.

3.5. Clinical non-response to Beva correlates with BMAL1 SNPs in CRC

Finally, the impact on the clinical outcome of four single nucleotide polymorphisms (SNPs) in the BMAL1 (*ARNTL*) gene was evaluated in

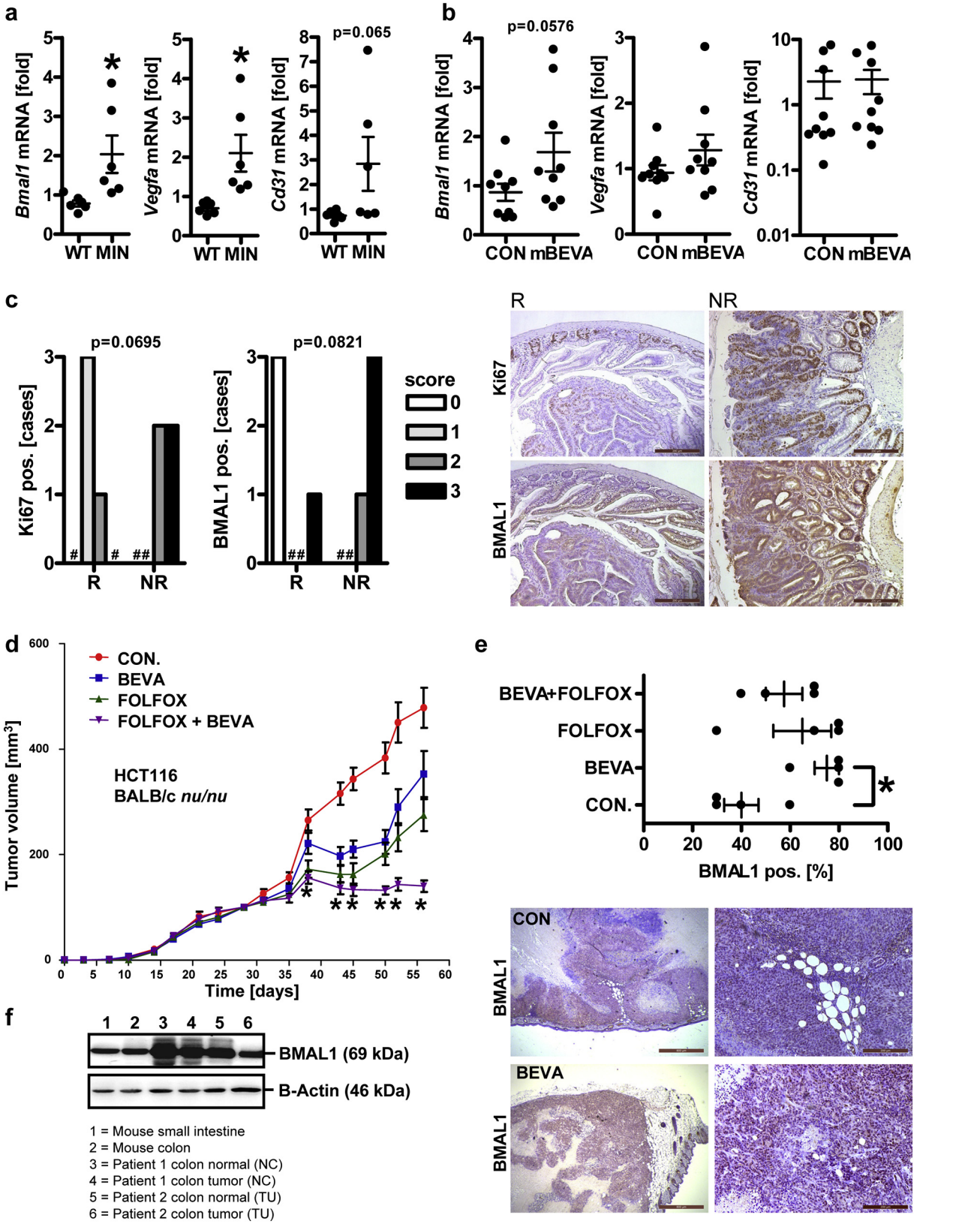

Fig. 2. BMAL1 detects murine CRCs resistant to mBeva therapy. (a) *Bmal1(Arntl)* mRNA is up-regulated in tumour-bearing mice. Total RNA was extracted from frozen small intestinal (SI) tissue of wild-type (WT) and *Apc* $^{min/+}$ (MIN) mice ($n = 6$ per group). CT-values from RT-qPCRs normalised to beta-2-microglobulin (*B2m)* are calculated as -fold ± S.E. ($^*p < .05$, Mann Whitney test). (b) mBeva fails to reduce *Bmal1* mRNA ($p = .0576$, Kruskal Wallis test) in tumour-bearing mice. Total RNA was extracted from colon tissue of untreated and mBeva-treated *Apc* $^{min/+}$ mice ($n = 9$ per group). RT-qPCRs were analysed as in panel a. (c) Non-response to mBeva correlates with high Ki67 ($p = .0695$ Fisher Exact test; $^*p = .0170$ t-test) and BMAL1 ($p = .0821$ Fisher Exact test; $^*p = .0447$ t-test) protein expression in *Apc* $^{min/+}$ CRCs. IHC staining positivity scores are from absolute animal numbers [cases] ($n = 4$ per group, NR *vs.* R). NR = non-responder; R = responder; # = no case recorded. Quantitative analyses (left) and representative images (right, original magnification 100×). (d) Beva and FOLFOX in combination inhibit tumour growth in BALB/c $^{nu/nu}$ mouse xenograft CRCs compared to monotherapy. Animals were injected (s.c.) with HCT116 cells, and, after 37 days, treated once per week (i.p) with vehicle (CON.), Beva (10 mg/kg) or FOLFOX (40 mg/kg 5-FU, 3.4 mg/kg oxaliplatin, 13.4 mg/kg folinic acid) or in combination (Beva given 24 h later than FOLFOX) for 4 weeks. Tumour volumes [in mm^3] are means ± S.E. ($n = 12$ per group, $^*p < .001$ FOLFOX+Beva *vs.* vehicle control, t-test). (e) Beva fails to reduce BMAL1 protein in mouse xenografts. IHC staining frequency from CRC xenografts (in panel d) is calculated in % ± S.E. ($n = 4$ per group,$^*p = .0286$ Beva *vs.* vehicle control, Mann Whitney test). Quantitative analyses (top) and representative images (bottom, original magnifications 25×, 100×). (f) Detection of BMAL1 protein in tissue lysates from murine or human normal colon (NC) and CRC (TU). Representative Western blots.

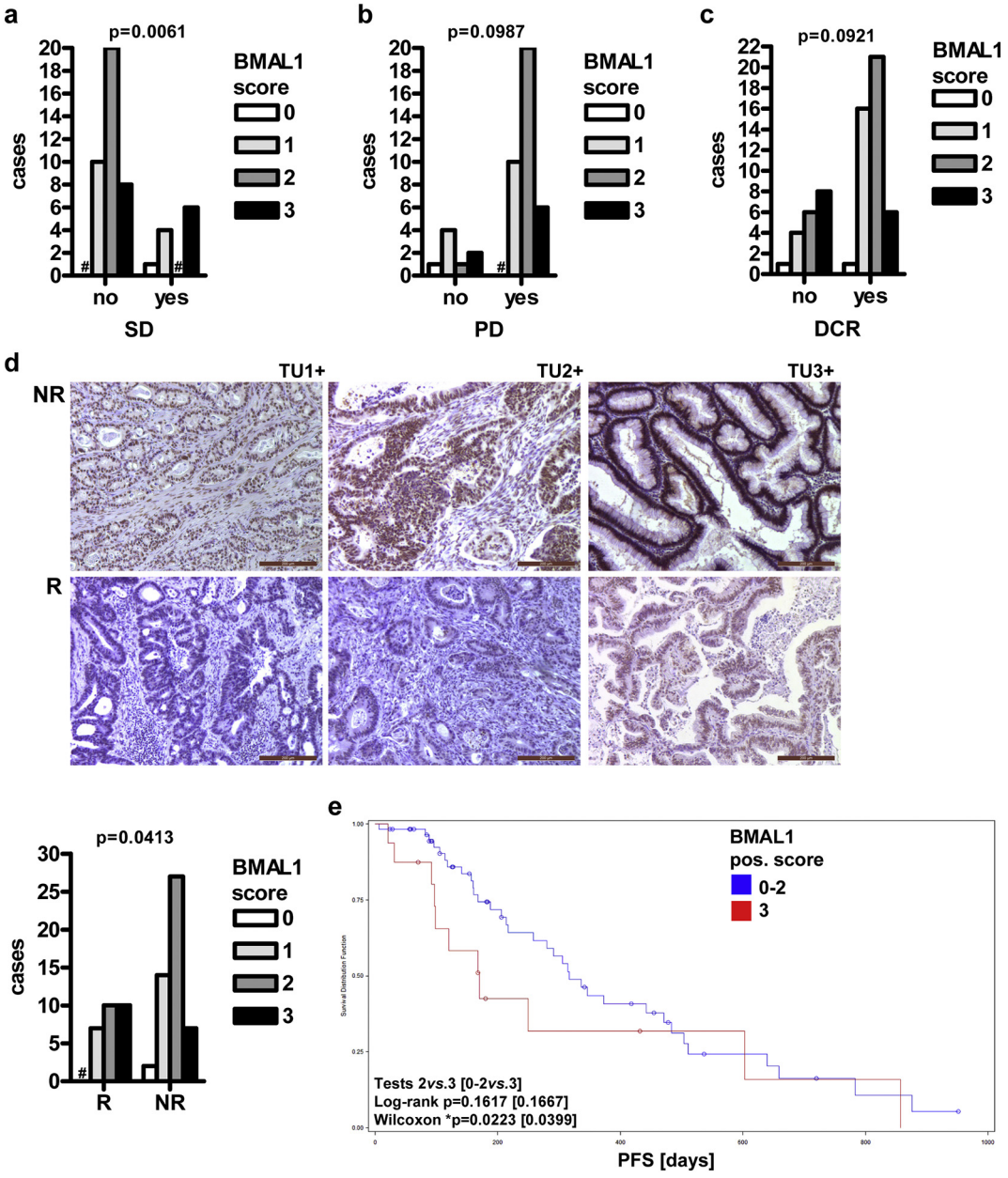

Fig. 3. Clinical non-response to Beva correlates with BMAL1 in human CRC. Associations of BMAL1 protein expression in tumour cells of CRC patients with clinical outcome after Beva treatment (# = no case recorded). Detailed statistics for clinical parameters is shown in Supplementary Tables 7–10. (a) BMAL1 negatively correlates with SD [SD *vs.* non-SD (=PD); $n = 44$ cases; scores 0–3: Cochran Armitage trend test $^*p = .0061$; scores 0/1 *vs.* 2/3: Fisher Exact test $^*p = .0130$]. (b) BMAL1 positively correlates with PD [PD *vs.* non-PD (=PR/SD); n = 44 cases; scores 0/1 *vs.* 2/3: Fisher Exact test $p = .0987$]. (c) BMAL1 negatively correlates with DCR [R (PR/SD) *vs.* NR (PD); $n = 63$ cases; scores 0–3: Cochran Armitage trend test $p = .0921$]. (d) BMAL1 positively correlates with poor clinical outcome [R (PR/SD) *vs.* NR (PD/Death); $n = 77$ cases; scores 0/1/2 *vs.* 3: Fisher Exact test $^*p = .0413$]. Response definition by PFS [cut-off: NR < 10 months > R]. Patient-wise outcomes according to RECIST [20] are shown in Supplementary Fig. 4. Representative images (top, original magnification 100×) and quantitative analyses (bottom). (e) BMAL1 correlates with reduced PFS. Kaplan-Meier curves were calculated from the first observed progress (PD) according to RECIST: [$n = 74$ cases; scores 2 *vs.* 3: $p = .1617$ log rank test HR = 1.687 (95% CI 0.79–4.18), $^*p = .0223$ Wilcoxon test; scores 0–2 *vs.* 3: $p = .1667$ log rank test HR = 1.601 (95% CI 0.79–3.84), $^*p = .0399$ Wilcoxon test]. Additional pair-wise comparisons are presented in Supplementary Fig. 6.

mCRC patients (TU, $n = 215$) treated with first-line FOLFIRI plus Beva in the randomised phase III TRIBE trial [21,22]. Baseline patient and tumour characteristics are listed in Supplementary Table 12. Three of the SNPs were in introns, while *rs2279287* located to the upstream (promoter) regulatory region of the gene (Supplementary Table 2). Among the evaluated SNPs, *rs11022780* showed a significant association with overall survival (OS) (Fig. 4a). Patients with any C allele had a shorter median OS than those harboring T/T allele (25.0 *vs.* 32.9 months) both in univariate (HR = 1.63, 95% CI 1.14–2.32, $^*p = .006$) and multivariable (HR = 1.61, 95% CI 1.10–1.62, $^*p = .014$) analysis. This effect was significant in the subgroup analysis for tumour location (Fig. 4a) and *RAS* mutational status (Supplementary Fig. 8a). Notably, *rs2279287, rs7938307* and *rs7396943* SNPs revealed significant associations with a shorter PFS in subgroups by gender, tumour location or *RAS* mutational status (Fig. 4b, Supplementary Fig. 8b-c). Results from interaction tests for SNPs and gender, tumour location and *RAS* status are summarised in Supplementary Table 13. The association of SNPs with outcome in the overall patient cohort is presented in Supplementary Table 14, while significant results of subgroup analyses are reported in Supplementary Table 15.

In summary, BMAL1 (*ARNTL*) gene alteration(s) and high protein expression correlated with unfavourable clinical outcomes in CRC patients treated with Beva. Overall, BMAL1 seems to act as a "bad guy" conferring resistance to Beva, both in mice and humans.

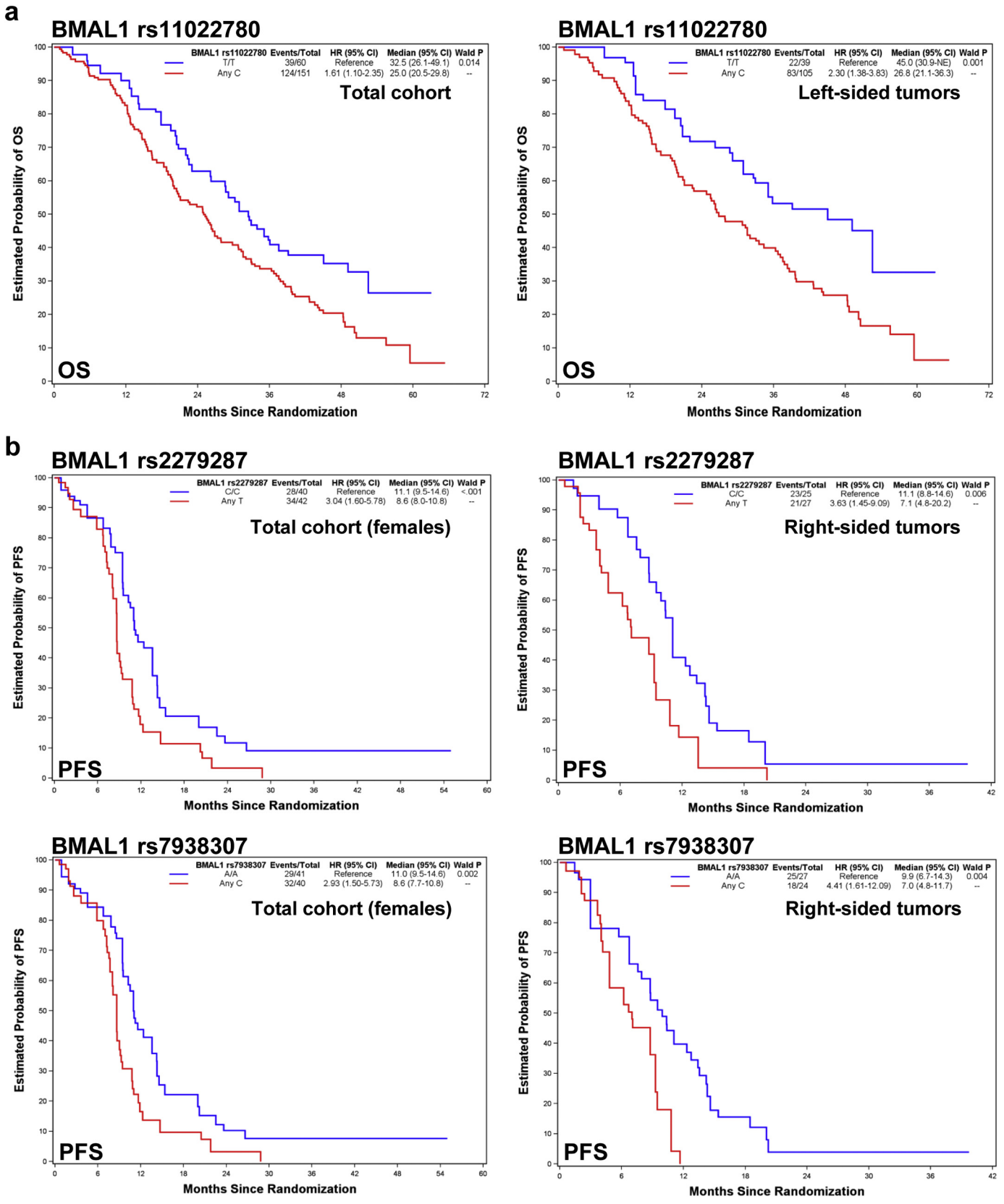

Fig. 4. Clinical non-response to Beva correlates with BMAL1 SNPs in human CRC. SNPs in the BMAL1 (*ARNTL*) gene correlate with poor prognosis and clinical response in CRC patients of the phase III TRIBE cohort [21,22]. Significant results of adjusted Kaplan-Meier plots by months are shown. Events/total, HR, median and Wald *P*-value were based on the multivariable Cox proportional hazards regression model as detailed in *Materials & Methods*. Complete statistics is presented in Supplementary Tables 12–15. (a) SNP *rs11022780* is associated with shortened OS in the total population and upon subgroup analysis for tumour location. (b) SNPs *rs2279287* and *rs7938307* are associated with shortened PFS upon subgroup analysis for gender and tumour location.

3.6. REVERBA binds to a RORE-like element in the human VEGFA promoter

To decipher the molecular mechanism, underlying the observed *in vivo* resistance to Beva in presence of BMAL1, two human CRC cell lines (SW480, HCT116) with activating mutations in Wnt/Ras-signalling pathway components (such as in *APC* and *KRAS*) were chosen as *in vitro* models for the *Apc* $^{min/+}$ GEMM and the majority of human CRCs (CMS2/3) [29].

BMAL1 is an activator of *REVERBA* [7,8] and *VEGFA* [6,39] gene transcription. We therefore hypothesised that the two transcription factors may be mechanistically connected in mediating Beva resistance. To this end, we first performed an *in silico* search using AliBaba2.1 for RORE-like motifs in the proximal (−2 kb) promoter of the human *VEGFA* gene. Two putative RORE sites (−1464 bp; −672 bp) were identified in proximity to a cognate BMAL1 binding site (E-box) (−1688 bp) [6,39] and estrogen receptor-responsive element (ERE) (−1542 bp) [40] (Fig. 5a, Supplementary Fig. 9). To test for DNA-binding, we amplified the predicted ROREs by PCR upon chromatin immunoprecipitation (ChIP) of the endogenous human *VEGFA* promoter. Cells (SW480, HCT116) were transfected with empty vector (EV) or REVERBA expression plasmid for 48 h, followed by ChIP. REVERBA Ab pulled-down DNA harboring the −672 bp RORE (Fig. 5b) (~2-fold; $^*p < .05$ *vs.* no Ab control, Mann Whitney test, $n = 4$–5 per cell line), but not the −1464 bp RORE. Nuclear extracts from SW480 cells transfected with EV or REVERBA were incubated with biotin-labelled oligonucleotides containing the predicted ROREs. Electrophoretic mobility shift assay (EMSA) (Fig. 5c) confirmed binding of ectopic REVERBA to wild-type −672 bp RORE (~10-fold; $^*p < .05$ *vs.* EV, Two-way ANOVA, $n \geq 3$ per cell line), but not to the mutant probe.

The upstream region of the human *VEGFA* gene, covering -2 kb until the start of the protein coding sequence, was then inserted into pGL3 luciferase reporter plasmid and transfected into SW480 cells for 48 h (Fig. 5d). REVERBA overexpression increased luciferase activity driven by the -2 kb *VEGFA* promoter (3.6 ± 0.3 *vs.* 1.1 ± 0.1 $^*p < .05$ -fold *vs.* EV, Mann Whitney test, $n = 3$ per cell line). Similar results were obtained from HCT116 and HEK293T (as non-cancer control) cells (Supplementary Fig. 10). These data indicated that REVERBA binds and transactivates the human *VEGFA* promoter.

3.7. REVERBA cooperates with BMAL1 to increase VEGFA synthesis

To elucidate whether DNA-binding translates into expression of the endogenous *VEGFA* gene, SW480 cells were transfected with EV or REVERBA for 48 h, followed by RNA extraction and RT-qPCR analysis. Notably, REVERBA overexpression increased *VEGFA* mRNA (by 70%; $^*p < .05$ *vs.* EV, One-sample *t*-test, $n = 3$) (Fig. 5e). ELISA confirmed augmented VEGFA secretion into the extracellular milieu upon overexpression of REVERBA (SW480: 82 ± 3 *vs.* 54 ± 5 pg/ml, $^*p < .05$ *vs.* EV, Paired t-test; $n = 3$) (Fig. 5f). The positive effect of REVERBA on endogenous VEGFA expression was most prominent in SW480 cells, possibly due to already high basal VEGFA levels in HCT116 (555 ± 47 *vs.* 519 ± 13 pg/ml) and HEK293T (305 ± 23 *vs.* 165 ± 10 pg/ml) cells (Supplementary Fig. 10).

To interrogate the role of REVERBA in the regulation of VEGFA synthesis, we selected BMAL1 which, similar to MYC [12], binds to *E*-boxes adjacent to the predicted RORE [40] and up-regulates *VEGFA* transcription [7,8]. Indeed, BMAL1 overexpression in SW480 cells increased *VEGFA* promoter activity (Fig. 5g), *VEGFA* mRNA (Fig. 5h) and VEGFA protein (Fig. 5i). BMAL1 also augmented *VEGFA* promoter activity in combination with REVERBA (Fig. 6a). Similar results were obtained from HCT116 and HEK293T cells (Supplementary Fig. 11). Thus, REVERBA seems to cooperate with BMAL1.

3.8. REVERBA and BMAL1 confer mBeva resistance in human CRC cells

VEGFA stimulates its own expression *via* VEGFA receptor-2 (VEGFR2) in a para- and autocrine fashion [40,41]. To test if neutralization of VEGFA by mBeva interrupts this positive amplification loop, cells (SW480, HCT116, HEK293T) were transfected with EV, REVERBA or BMAL1 together with -2 kb *VEGFA* promoter reporter plasmid for 24 h, followed by 48 h incubation in starvation (SM) or conditioned (CM) medium in absence or presence of mBeva (10 μg/ml) (Fig. 6b). Media preparation is described in *Materials & Methods*. Baseline luciferase activity was measured upon cultivation in SM and compared to the one achieved by CM, which, due to its cocktail of secreted growth factors (including VEGFA), served as a stimulant for the signalling response tested. REVERBA and BMAL1 increased the reporter activity under all conditions, whereas mBeva was unable to dampen this response ($^*p < .05$ *vs.* EV, Two-way ANOVA, $n = 3$ per cell line).

To gain insight into related oncogenic pathways in addition to VEGFA, cells (SW480, HCT116) were transfected with REVERBA or BMAL1 together with reporter plasmids (Supplementary Fig. 12) detecting hypoxia, Ras or Wnt signalling. After 24 h, cells were serum-deprived (in SM) or stimulated (in CM) with or without mBeva (10 μg/ml) for additional 48 h (as described for Fig. 6b). REVERBA and BMAL1 increased hypoxia- and Wnt-driven luciferase activity, while Ras-signalling was preferentially augmented by REVERBA ($^*p < .05$, Two-way ANOVA, pair-wise subgroup analysis by Bonferroni post-tests as indicated by asterisks, $n = 3$ per plasmid and cell line). Again, mBeva did not significantly abrogate responses elicited by the two transcription factors in CM-stimulated cells as compared to the baseline of SM-exposed cells.

3.9. REVERBA inhibition, but not mBeva reduces proliferation of human CRC cells

The data above indicates that interference with REVERBA-BMAL1 signalling may be superior to VEGFA neutralization. To test this hypothesis, colorimetric MTT assays were performed to examine cell proliferation. SW480 cells were transfected with EV or REVERBA and cultivated for 1–7 days. REVERBA overexpression accelerated cell growth (~2-fold; $^*p < .05$ *vs.* EV, Two-way ANOVA, $n = 3$) (Fig. 7a), whereas REVERBA knock-down by siRNA reduced proliferation (Fig. 7b). When cells were incubated in presence of hemin (30 μM), a physiological modulator of REVERBs and other heme-binding proteins [31], growth was also diminished (by 80%; $^*p < .05$ *vs.* vehicle, Two-way ANOVA, $n = 3$) (Fig. 7c). In contrast, mBeva did not alter proliferation rates (Fig. 7d). Likewise, BMAL1 overexpression or knock-down *per se* remained ineffective (not shown). Thus, targeting REVERBA, a feedback regulator of BMAL1, may have a greater effect on tumour cell growth compared with VEGFA neutralization.

Taken together, these results suggest that REVERBA, indirectly, *e.g. via* cooperation with BMAL1, facilitates a feed-forward amplification loop [7,8], which culminates in augmented VEGFA synthesis (as depicted in Fig. 8). This sequence of events may underpin a vicious cycle insensitive to mBeva, but instead susceptible to REVERBA-BMAL1 inhibition.

4. Discussion

In this work, we provide evidence that BMAL1 is a functional modulator and potential biomarker of resistance to anti-angiogenic therapy in CRC. This conclusion was elaborated using a translational approach combining preclinical, clinical and cellular mechanistic studies.

Consistent with other reports on VEGFA-pathway inhibition [42,43], Beva reduced CRC growth in two independent mouse models which were driven by active Wnt/Ras-signalling and, thereby, resemble the most common consensus molecular subtypes (CMS2/3) of human CRC [29]. However, instead of reducing vessel density, stromal reactions prevailed (*e.g.* desmoplasia, fibrosis) and bowel inflammation was mitigated. Uncoupling of tumour growth from angiogenesis may be caused by differential sensitivity towards or dependency on VEGFA, as a growth and survival factor in a given cell type [42,43]. Thus, beyond tumour and

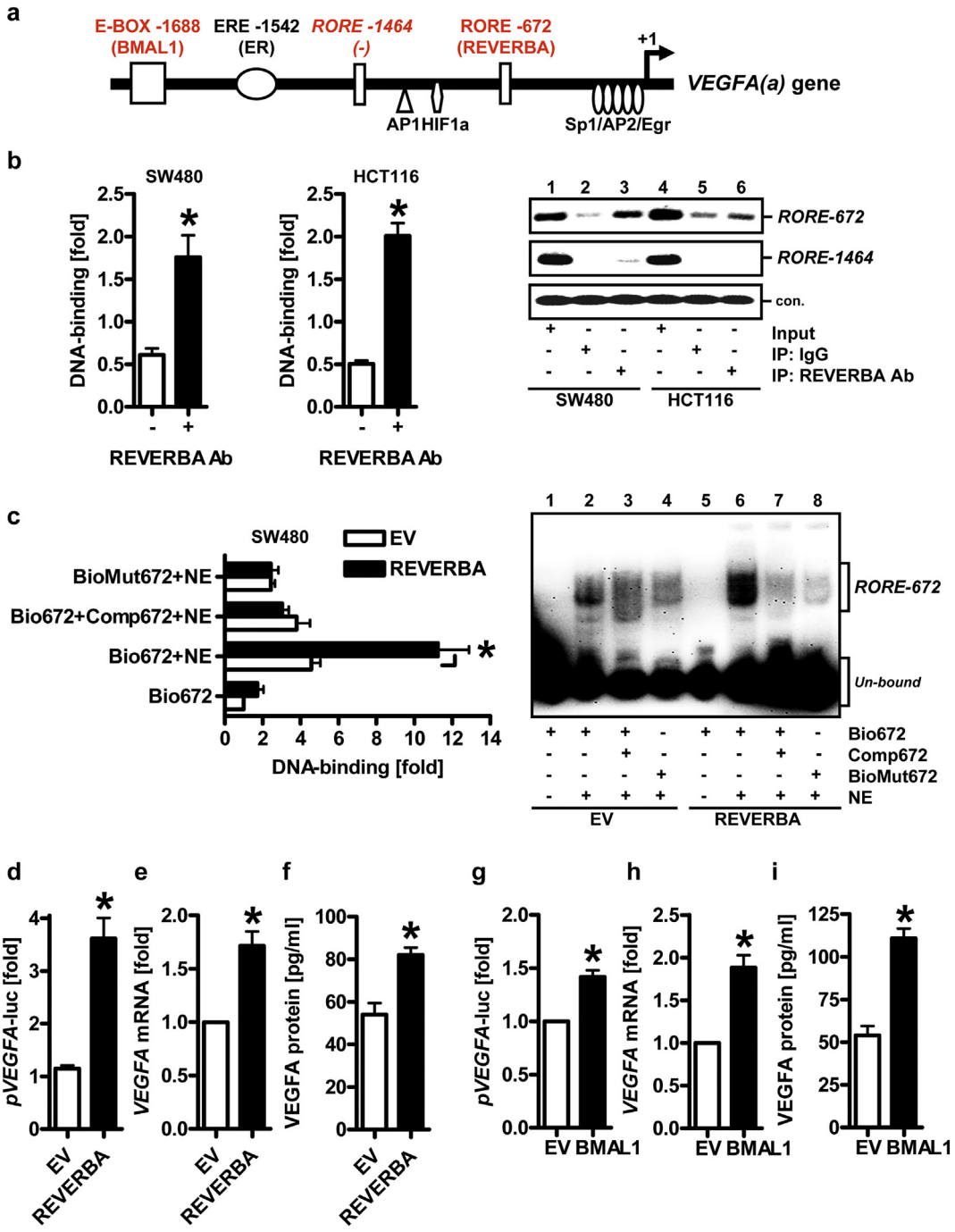

Fig. 5. REVERBA binds to a RORE-like element in the human *VEGFA* promoter. (a) Scheme of the human *VEGFA* promoter with RORE-like binding elements adapted from [40]. ERE = estrogen receptor-responsive element (−1542 Bp); RORE = predicted ROR/REVERB-responsive elements (−672 Bp; −1464 Bp); E-Box = BMAL1/MYC-binding element (−1688 Bp). (b) REVERBA binds to the -672RORE in the -2 kb human *VEGFA* promoter. SW480 and HCT116 cells were transfected with empty vector (EV) or REVERBA expression plasmid for 48 h, and chromatin-immunoprecipitation (ChIP) was performed using REVERBA Ab for IP and genomic qPCR for amplification of bound DNA. Left: CT-values normalised to *B2M* (on input DNA) were calculated as -fold ± S.E. (*$p < .05$ *vs.* no Ab control, Mann Whitney test, n = 4–5 per cell line). Right: Representative ethidium bromide-stained agarose gel of genomic PCRs. (c) REVERBA binds to wildtype (WT) but not mutant (MUT) -672RORE. SW480 cells were transfected as in panel b, and electrophoretic mobility shift assay (EMSA) was performed using biotin-labelled (or unlabelled oligonucleotides as competitors) and nuclear extracts. Left: O.D. values of gel-shifted bands were calculated as -fold ± S.E. (*$p < .05$ *vs.* EV, Two-way ANOVA, $n \geq 3$ per cell line). Right: Representative images from native SDS-PAGE. WT = -672RORE_pVEGFA; MUT = -672RORE_pVEGFAmut. (d–i) REVERBA and BMAL1 increase VEGFA synthesis in human CRC cells. d&g, *VEGFA* promoter activity. SW480 cells were transfected with EV, REVERBA or BMAL1 expression plasmids, respectively, together with -2 kb human *VEGFA* promoter reporter plasmid for 48 h. Luciferase activity was normalised to protein content and expressed as -fold ± S.E. (*$p < .05$ *vs.* EV, Mann Whitney test, $n = 3$). e&h, *VEGFA* mRNA. Cells were transfected as in panel d, followed by extraction of total RNA. CT-values of RT-qPCRs were normalised to *B2M* and calculated as -fold ± S.E. (*$p < .05$ *vs.* EV, One-sample *t*-test, n = 3). f&i, VEGFA protein. Cells were transfected as in panel d. ELISA detecting soluble VEGFA protein was conducted on supernatants collected from monolayers. O.D. values were calculated from standards in pg/ml and presented as means ± S.E. (*$p < .05$ *vs.* EV, paired t-test, n = 3).

endothelial cells, other components of the tumour microenvironment, *e.g.* fibroblasts, macrophages or pericytes, may regulate VEGF signalling and secretion, and, thereby, contribute to the efficacy of Beva on CRC growth *in vivo*.

Previously recognised phenotypes in GEMMs confirm the co-existence of systemic cardio-vascular *vs.* local epithelial effects of BMAL1-dependent target genes (including *VEGFA*) [7,8]: As such, BMAL1 controls proliferation and migration of mesenchymal, neuronal,

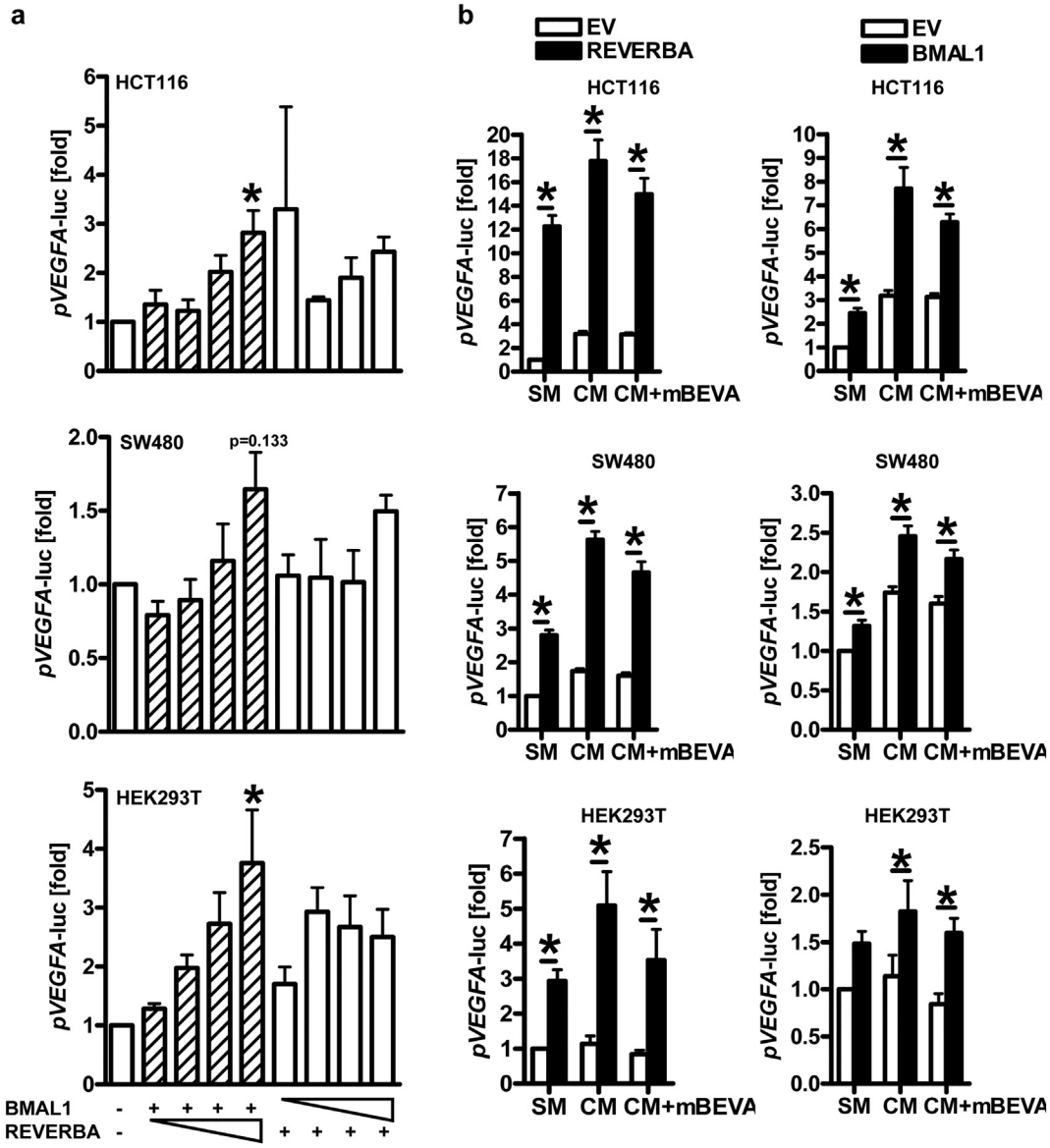

Fig. 6. REVERBA cooperates with BMAL1 to increase VEGFA synthesis. (a) REVERBA further increases *VEGFA* promoter activity driven by BMAL1. Cells (SW480, HCT116, HEK293T) were co-transfected for 48 h with -2 kb *VEGFA* promoter reporter plasmid together with EV (minus = 1 μg) or increasing amounts of REVERBA expression plasmid (triangle = 0, 0.5, 1, 2 μg) in combination with a fixed amount of BMAL1 expression plasmid (plus = 1 μg), or *vice versa*. Total DNA was adjusted to 4 μg per well of a 6-well plate. Data were analysed as in Fig. 5 (*p < .05 *vs.* EV, Two-way ANOVA, n = 3 per cell line). (b) mBeva is unable to reduce *VEGFA* promoter activity driven by REVERBA or BMAL1. Cells (SW480, HCT116, HEK293T) were transfected with EV, REVERBA or BMAL1 expression plasmids, respectively, together with the -2 kb *VEGFA* promoter reporter plasmid. After 24 h, cells were incubated with or without mBeva (10 μg/ml) in starvation medium (SM) or conditioned medium (CM) for additional 48 h. Media were prepared for each cell line, respectively, as detailed in *Materials & Methods*. Luciferase activity was normalised to protein content and expressed as -fold ± S.E. (*p < .05 *vs.* EV, Two-way ANOVA, n = 3 per cell line).

epidermal and intestinal stem cells, thereby governs initiation and progression of tumours [44,45]. BMAL1 is also required for growth and survival of bone marrow and leukemic stem cells [46]. We were unable to detect major signs of necrosis or apoptosis in Beva-treated tumours. Instead, Ki67 data indicates that reduced proliferation of cancer (stem) cells is one mechanism whereby neutralization of VEGFA inhibits tumour growth in mice, and this process may be counteracted by a gain of function in BMAL1.

In both CRC mouse models, Beva failed to attenuate or even further up-regulated BMAL1 expression during treatment. Thus, high BMAL1 expression in murine CRCs may be a drug-mediated passenger effect, but not necessarily the causative driver of resistance to Beva. Experimental studies in *Bmal1* transgenic or knock-out mice are required to further address this issue.

Our preclinical studies were confirmed by molecular and genomic analyses which revealed that SNPs in the BMAL1 (*ARNTL*) gene and high BMAL1 expression in tumour cells correlated with unfavourable clinical outcome in CRC patients that underwent combination chemotherapy with Beva. Compensatory up-regulation of alternative pro-angiogenic ligands and/or receptors in response to treatment have been postulated [2,47]. For example, additional VEGFA isoforms as well as VEGFB/C/D or placental growth factor allow by-passing of VEGFA-VEGFR2 signalling. Likewise, Notch signalling *via* delta-like ligand-4 evokes resistance by increasing VEGFR1 expression in the tumour-adjacent stroma [2]. Consistently, our data propose that resistance to Beva may be caused by intrinsic, intracellular "escape" pathways in tumour (stem) cells involving BMAL1 (and presumably other transcription factors) which lead to continuous VEGFA synthesis and secretion followed by persistent auto/paracrine stimulation of membrane-bound VEGFA-VEGFR2 signalling. Regarding the possible survival effects, one may speculate whether local gain of BMAL1-driven VEGFA production in tumour cells translates to other

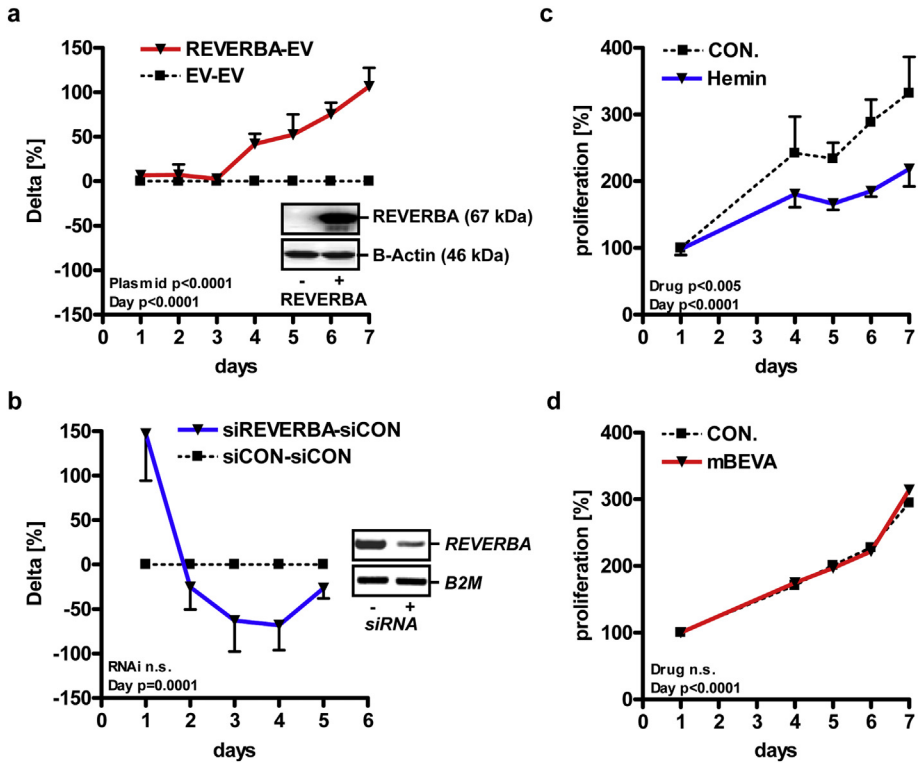

Fig. 7. REVERBA increases proliferation of human CRC cells. (a) REVERBA overexpression increases proliferation. SW480 cells were transfected with EV or REVERBA plasmid, and proliferation was measured by colorimetric MTT assay after 1 to 7 days. O.D. values were calculated in % compared with day 1 and presented as differences (Delta) of the means ± S.E. (*p < .05 EV *vs.* REVERBA, Two-way ANOVA, n = 3). Insert: Representative images of overexpressed REVERBA protein from Western blots. (b) REVERBA knock-down decreases proliferation. SW480 cells were transfected with REVERBA siRNA and control siRNA oligonucleotides as in panel a (n.s. siREVERBA *vs.* siCON.; Two-way ANOVA, n = 3). Insert: Representative images of ethidium bromide-stained agarose gels from RT-PCRs visualizing knock-down of *REVERBA* mRNA. (c) Hemin reduces proliferation. SW480 cells were grown in presence of vehicle control (DMSO) or hemin (30 μM) for the indicated times. Data from MTT assays were calculated in % compared with day 1 and presented as means ± S.E. (*p < .05 Hemin *vs.* control, Two-way ANOVA, n = 3). (d) mBeva is unable to reduce proliferation. SW480 cells were incubated without (control) or with mBeva (10 μg/ml) for the indicated times. Data from MTT assays were calculated as in panel c (n.s., mBeva *vs.* control, Two-way ANOVA, n = 3).

VEGFA-sensitive stroma cell types in the microenvironment, including endothelial cells, and/or even spreads systemically *via* the vasculature.

Despite paying attention to exact daily timing of injections and endpoints in our preclinical studies, we cannot exclude circadian variations due to different sampling times of human tissues during routine surgery in the hospital. Future synchronised studies are warranted to address this limitation. In this context, the biological significances of the SNPs in the BMAL1 (*ARNTL*) gene in CRC remain to be defined as well. Clinical associations exist for sleep-wake disturbance in Alzheimer's disease [48], bipolar disorder and seasonal depression [49] and metabolism [50] (Supplementary Table 2). Whether these SNPs evoke a gain or loss of BMAL1 expression and/or an altered protein function similar to mutations in oncogenic driver genes, such as KRAS in CRC [29], remains an open question. All the described SNPs locate to upstream regulatory regions (promoter/5'-UTR) or non-coding introns, presumably resulting in altered mRNA transcription/splicing/stability or alternative mRNA/translation variants. To answer these questions, SNPs have to be sequenced, amplified and inserted into appropriate expression vectors for further functional studies in cell and *in vivo* models.

To in part explain the observed *in vivo* phenotypes and clinical data, we have proposed a mechanistic model in human CRC cells (Fig. 8), in which BMAL1 increases VEGFA expression together with REVERBA. However, the apparent positive effect of REVERBA on VEGFA synthesis appears to be indirect, comprising so far unknown epigenetic de-repression mechanisms through cooperation with BMAL1 and other transcription factors or co-activators [51]. Despite lacking the N-terminal transactivation function common in nuclear receptors, REVERBA interacts with enzymes [52] or DNA-bound factors, such as NFκB [53], Sp1 [54] or NF-Y [55], to indirectly modulate transcription. REVERBA is itself subjected to post-translational modifications or release of co-repressors [7,8], resulting in "repression of the repressor". Hence, our case most likely implies an indirect mode of action, where REVERBA binds to the RORE adjacent to the *E*-box [40] recognised by BMAL1 in the *VEGFA* promoter to positively influence transcription.

In line with our findings in mice and patients, these molecular data suggest a positive amplification loop where VEGFA Ab fails to disrupt REVERBA/BMAL1-driven VEGFA-VEGFR2 signalling in tumour cells. This failure could be caused by an overabundance of secreted VEGFA which simply overwhelms the capacity of Beva to neutralize this growth factor produced by the intracellular transcription machinery (Fig. 8). In addition, REVERBA and BMAL1 (presumably together with non-clock transcription factors [9]) augmented transcriptional responses to major oncogenic drivers of human CRC (such as Wnt and Ras) [29].

These cooperative mode of action integrates well into previous evidence on BMAL1 regarding chemotherapy responsiveness: BMAL1 forms heterodimers with CLOCK or NPAS2 (and non-clock factors [9]) to regulate genes involved in DNA-repair, cell cycle checkpoints (p53 e.a.), cytoskeleton reorganization and drug metabolism. Many chemotherapeutics evoke DNA-damage (*e.g.* bulky adducts, double strand breaks). As such, BMAL1 protects against toxicity of cyclophosphamide [56], cisplatin and doxorubicin [57], while it sensitises to paclitaxel [58], gemcitabine [59] and oxaliplatin [60] in cells, mice or patients. Further, BMAL1 cooperates with p53 to protect cells from UV stress-induced DNA-damage [61]. Clock-related gene expression also predicts clinical response to neoadjuvant chemoradiation in rectal cancer patients [62]. Hence, BMAL1-dependent regulation of DNA-repair mechanisms seems to be one common underlying mechanism how resistance *vs.* sensitivity to (radio)chemotherapy is established. So far, functional connections of BMAL1 with clinical response against targeted therapies (*e.g.* cetuximab in CRC) have not been described. Future studies are required

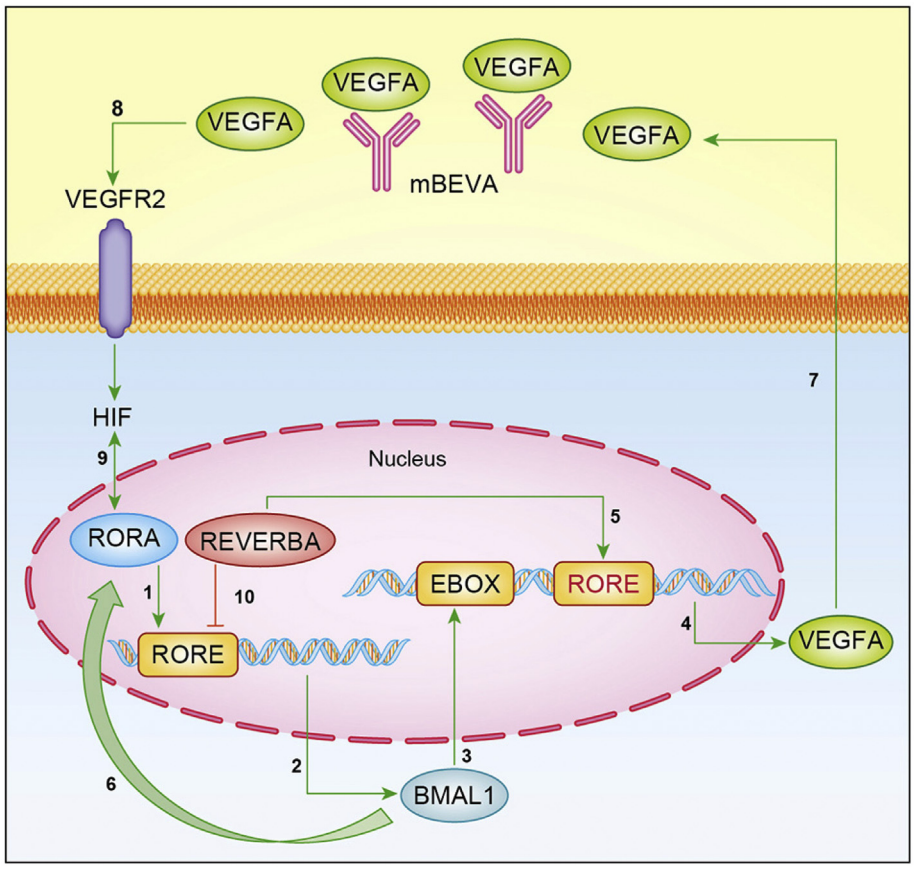

Fig. 8. Model of REVERBA-BMAL1-VEGFA signalling in CRC. Data on transcription factor binding sites and pathways are integrated from the literature [7,8] and own experiments. 1 = RORA binds to the canonical RORE in the BMAL1 (*ARNTL*) promoter, 2 = RORA induces BMAL1 mRNA transcription, 3 = BMAL1 binds to the *E*-Box in the *VEGFA* promoter, 4 = BMAL1 induces *VEGFA* mRNA transcription, 5 = REVERBA binds to the predicted RORE in the *VEGFA* promoter and (presumably *via* an indirect de-repression mechanism) contributes to BMAL1-driven *VEGFA* mRNA transcription, 6 = BMAL1 activates transcription of *RORA* mRNA *via* E-Boxes in the *RORA* promoter further amplifying BMAL1 levels (and may cooperate with non-circadian clock transcription factors [9] to regulate additional genes involved in cell proliferation, DNA-repair e.a.), 7 = VEGFA is secreted from cells, 8 = VEGFA binds to VEGFR2 on the same or adjacent cells, 9 = VEGFR2 signalling activates HIF1A which binds to the HRE in the *RORA* promoter and induces *RORA* transcription, completing the feed-forward circle, 6 and 10 = BMAL1 induces *REVERBA* transcription *via* E-Boxes in the *REVERBA* promoter, REVERBA then binds to the canonical RORE in the *BMAL1* promoter and inhibits *BMAL1* transcription, establishing a negative feed-back leverage; green = activation, red = inhibition. mBeva fails to interrupt this interlocked amplification circuits, thereby establishing a potential vicious feed-forward cycle resulting in resistance to VEGFA-neutralizing Ab treatment in human CRC cells.

to elucidate whether the impact of BMAL1 [57] on therapy outcome is specific for a given intervention modality or tumour context.

Pharmacological re-entrainment of the circadian clock in cancer cells improves tumour control, *e.g.* by seliciclib in mice [63] or cortisol in patients [64]. Likewise, cancer chronotherapy, the daily timing of chemotherapeutics administration (such as irinotecan) determines tolerability and clinical outcome [65]. In mice, REVERBA and BMAL1 were the best discriminators for chronotoxicity [66]. BMAL1, *per se* or *via* REVERBA, may be therefore proposed as a potential druggable target for preventing resistance to Beva in human CRC. CRY stabilisers have been developped, *e.g.* KL001, which inhibit the activity of BMAL1 [67]. REVERBA-agonists (SR9009/SR9011) exert strong cytotoxicity and facilitate oncogene-induced senescence in cell and mouse cancer models [68,69]. REVERBB-antagonist ARN5187 inhibits autophagy and reduces viability in breast cancer cells [70]. Consistently, we found that proliferation of CRC cell lines was attenuated by REVERBA siRNA and hemin, a physiological modulator of heme-binding proteins beyond REVERBs [31]. Thus, pharmacological intervention at the interlocked feed-back loops of circadian rhythm transcription factors may represent an attractive approach to target cancer.

In conclusion, our data demonstrate that BMAL1 is frequently expressed in tumour tissues from CRC patients refractory to anti-VEGFA therapy with Beva. These data therefore support the monitoring of CRC patients for these markers, at the protein or genomic (SNP) level, to assess their risk for clinical non-response [18]. If combined with efficient screening procedures, biomarker-guided assessment may improve detection of early resistance and may prevent therapy failure.

Acknowledgements and funding sources

This study was supported by grants to EB from the Deutsche Krebshilfe (#108287 and #111086). FE received a fellowship from the "Studienstiftung des deutschen Volkes". JB was supported by the Translational Physician Scientist (TraPS) Program of the Medical Faculty Mannheim of the Heidelberg University. WW was awarded a fellowship from the Chinese Scholarship Council (#201408080116). ME was supported by the State of Baden-Württemberg for "Center of Geriatric Biology and Oncology (ZOBEL) – Perspektivförderung" and "Biology of Frailty - Sonderlinie Medizin". ATB and ME received fundings from the European Commission Seventh Framework Programme (Contract No. 278981 [ANGIOPREDICT]) and are supported by the European Commission Horizon 2020 Programme (Contract No. 754923 [COLOSSUS]). ATB is further supported by Science Foundation Ireland under grant 13/CDA/2183"Coloforetell". HJL was partly funded by the National Cancer Institute (grant number P30CA014089), the Gloria Borges WunderGlo Foundation-The Wunder Project, the Dhont Family Foundation, the San Pedro Peninsula Cancer Guild, the Daniel Butler Research Fund, and the Call to Cure Research Fund. The content is solely the responsibility of the authors and does not necessarily represent the official views of the National Cancer Institute or the National Institutes of Health.

Declaration of competing interests

The authors declare no conflicts of interest. The reagent mBeva was obtained on the basis of a material transfer agreement (MTA#10082012) from Roche Diagnostics GmbH (Penzberg, Germany). HJL has received clinical trial financial support from Merck Serono and Roche and honoraria for advisory board membership and lectures from Bayer, Boehringer Ingelheim, Genentech, Merck Serono and Roche. Part of the data were accepted as a poster presentation at the GI-ASCO conference 2017 and deposited as an abstract under the following link: *http://ascopubs.org/doi/abs/10.1200/JCO.2018.36.4_suppl.705*.

Author contributions

All authors contributed and critically reviewed and approved the manuscript. EB and ME defined the research theme. EB, FB, FE, FH, ISM and WW designed the methods and carried out the experiments. ATB, EB, FB, FE, FH, HJL, ISM and WW analysed the data and interpreted the results. CW, FB and HJL performed statistical calculations. AM, CAW, JK and TG conducted and analysed immunostainings. ATB, EB, FB and ISM drafted the manuscript. ATB, FL, HJL, JB, ME, NH, NS and RH provided samples and/or collected clinical data.

Writing assistance

None.

Appendix A. Supplementary data

Supplementary data to this article can be found online at https://doi.org/10.1016/j.ebiom.2019.07.004.

References

[1] Ferrara N, Hillan KJ, Gerber H-P, et al. Discovery and development of bevacizumab, an anti-VEGF antibody for treating cancer. Nat Rev Drug Discov 2004;3:391–400.
[2] De Palma M, Biziato D, Petrova TV. Microenvironmental regulation of tumour angiogenesis. Nat Rev Cancer 2017;17:457–74.
[3] Koyanagi S, Kuramoto Y, Nakagawa H, et al. A molecular mechanism regulating circadian expression of vascular endothelial growth factor in tumor cells. Cancer Res 2003;63:7277–83.
[4] Peek CB, Levine DC, Cedernaes J, et al. Circadian clock interaction with HIF1alpha mediates oxygenic metabolism and anaerobic glycolysis in skeletal muscle. Cell Metab 2017;25:86–92.
[5] Ma Z, Jin X, Qian Z, et al. Deletion of clock gene Bmal1 impaired the chondrocyte function due to disruption of the HIF1alpha-VEGF signaling pathway. Cell Cycle 2019:1–17.
[6] Jensen LD, Cao Z, Nakamura M, et al. Opposing effects of circadian clock genes bmal1 and period2 in regulation of VEGF-dependent angiogenesis in developing zebrafish. Cell Rep 2012;2:231–41.
[7] Dierickx P, Van Laake LW, Geijsen N. Circadian clocks: from stem cells to tissue homeostasis and regeneration. EMBO Rep 2018;19:18–28.
[8] Kojetin DJ, Burris TP. REV-ERB and ROR nuclear receptors as drug targets. Nat Rev Drug Discov 2014;13:197–216.
[9] Shostak A, Brunner M. Help from my friends-cooperation of BMAL1 with noncircadian transcription factors. Genes Dev 2019;33:255–7.
[10] Sahar S, Sassone-Corsi P. Metabolism and cancer: the circadian clock connection. Nat Rev Cancer 2009;9:886–96.
[11] Relogio A, Thomas P, Medina-Perez P, et al. Ras-mediated deregulation of the circadian clock in cancer. PLoS Genet 2014;10:e1004338.
[12] Altman BJ, Hsieh AL, Sengupta A, et al. MYC disrupts the circadian clock and metabolism in Cancer cells. Cell Metab 2015;22:1009–19.
[13] Sotak M, Polidarova L, Ergang P, et al. An association between clock genes and clock-controlled cell cycle genes in murine colorectal tumors. Int J Cancer 2013;132:1032–41.
[14] Huisman SA, Oklejewicz M, Ahmadi AR, et al. Colorectal liver metastases with a disrupted circadian rhythm phase shift the peripheral clock in liver and kidney. Int J Cancer 2015;136:1024–32.
[15] Karantanos T, Theodoropoulos G, Pektasides D, et al. Clock genes: their role in colorectal cancer. World J Gastroenterol 2014;20:1986–92.
[16] O'Halloran PJ, Viel T, Murray DW, et al. Mechanistic interrogation of combination bevacizumab/dual PI3K/mTOR inhibitor response in glioblastoma implementing novel MR and PET imaging biomarkers. Eur J Nucl Med Mol Imaging 2016;43:1673–83.
[17] Betge J, Barat A, Murphy V, et al. Outcome of colorectal Cancer patients treated with combination bevacizumab therapy: a pooled retrospective analysis of three European cohorts from the Angiopredict initiative. Digestion 2016;94:129–37.
[18] van Dijk E, Biesma HD, Cordes M, et al. Loss of chromosome 18q11.2-q12.1 is predictive for survival in patients with metastatic colorectal Cancer treated with bevacizumab. J Clin Oncol 2018;36:2052–60.
[19] Schlemper RJ, Riddell RH, Kato Y, et al. The Vienna classification of gastrointestinal epithelial neoplasia. Gut 2000;47:251–5.
[20] Schwartz LH, Litiere S, de Vries E, et al. RECIST 1.1-update and clarification: from the RECIST committee. Eur J Cancer 2016;62:132–7.
[21] Cremolini C, Loupakis F, Antoniotti C, et al. FOLFOXIRI plus bevacizumab versus FOLFIRI plus bevacizumab as first-line treatment of patients with metastatic colorectal cancer: updated overall survival and molecular subgroup analyses of the open-label, phase 3 TRIBE study. Lancet Oncol 2015;16:1306–15.
[22] Loupakis F, Cremolini C, Masi G, et al. Initial therapy with FOLFOXIRI and bevacizumab for metastatic colorectal cancer. N Engl J Med 2014;371:1609–18.
[23] Altman DG, McShane LM, Sauerbrei W, et al. Reporting recommendations for tumor marker prognostic studies (REMARK): explanation and elaboration. PLoS Med 2012;9:e1001216.
[24] Amos CI, Dennis J, Wang Z, et al. The OncoArray consortium: a network for understanding the genetic architecture of common cancers. Cancer Epidemiol Biomarkers Prev 2017;26:126–35.
[25] Friedrich T, Richter B, Gaiser T, et al. Deficiency of caveolin-1 in Apc(min/+) mice promotes colorectal tumorigenesis. Carcinogenesis 2013;34:2109–18.
[26] MacMillan CJ, Doucette CD, Warford J, et al. Murine experimental autoimmune encephalomyelitis is diminished by treatment with the angiogenesis inhibitors B20-4.1.1 and angiostatin (K1−3). PLoS One 2014;9:e89770.
[27] Liang WC, Wu X, Peale FV, et al. Cross-species vascular endothelial growth factor (VEGF)-blocking antibodies completely inhibit the growth of human tumor xenografts and measure the contribution of stromal VEGF. J Biol Chem 2006;281:951–61.
[28] Besenhard MO, Jarzabek M, O'Farrell AC, et al. Modelling tumour cell proliferation from vascular structure using tissue decomposition into avascular elements. J Theor Biol 2016;402:129–43.
[29] Guinney J, Dienstmann R, Wang X, et al. The consensus molecular subtypes of colorectal cancer. Nat Med 2015;21:1350–6.
[30] Mitamura T, Pradeep S, McGuire M, et al. Induction of anti-VEGF therapy resistance by upregulated expression of microseminoprotein (MSMP). Oncogene 2018;37:722–31.
[31] Vaissiere A, Berger S, Harrus D, et al. Molecular mechanisms of transcriptional control by rev-erbalpha: an energetic foundation for reconciling structure and binding with biological function. Protein Sci 2015;24:1129–46.
[32] Burgermeister E, Friedrich T, Hitkova I, et al. The Ras inhibitors caveolin-1 and docking protein 1 activate peroxisome proliferator-activated receptor gamma through spatial relocalization at helix 7 of its ligand-binding domain. Mol Cell Biol 2011;31:3497–510.
[33] Hitkova I, Yuan G, Anderl F, et al. Caveolin-1 protects B6129 mice against helicobacter pylori gastritis. PLoS Pathog 2013;9:e1003251.
[34] Ebert MP, Tanzer M, Balluff B, et al. TFAP2E-DKK4 and chemoresistance in colorectal cancer. N Engl J Med 2012;366:44–53.
[35] Friedrich T, Sohn M, Gutting T, et al. Subcellular compartmentalization of docking protein-1 contributes to progression in colorectal cancer. EBioMedicine 2016;8:159–72.
[36] Kather JN, Weis CA, Bianconi F, et al. Multi-class texture analysis in colorectal cancer histology. Sci Rep 2016;6:27988.
[37] Bais C, Mueller B, Brady MF, et al. Tumor microvessel density as a potential predictive marker for bevacizumab benefit: GOG-0218 biomarker analyses. J Natl Cancer Inst 2017;109.
[38] Cerami E, Gao J, Dogrusoz U, et al. The cBio cancer genomics portal: an open platform for exploring multidimensional cancer genomics data. Cancer Discov 2012;2:401–4.
[39] Jensen LD, Cao Y. Clock controls angiogenesis. Cell Cycle 2013;12:405–8.
[40] Pages G, Pouyssegur J. Transcriptional regulation of the vascular endothelial growth factor gene–a concert of activating factors. Cardiovasc Res 2005;65:564–73.
[41] Chatterjee S, Heukamp LC, Siobal M, et al. Tumor VEGF:VEGFR2 autocrine feed-forward loop triggers angiogenesis in lung cancer. J Clin Invest 2013;123:1732–40.
[42] Korsisaari N, Kasman IM, Forrest WF, et al. Inhibition of VEGF-A prevents the angiogenic switch and results in increased survival of Apc+/min mice. Proc Natl Acad Sci U S A 2007;104:10625–30.
[43] Goodlad RA, Ryan AJ, Wedge SR, et al. Inhibiting vascular endothelial growth factor receptor-2 signaling reduces tumor burden in the ApcMin/+ mouse model of early intestinal cancer. Carcinogenesis 2006;27:2133–9.
[44] Stokes K, Cooke A, Chang H, et al. The circadian clock gene BMAL1 coordinates intestinal regeneration. Cell Mol Gastroenterol Hepatol 2017;4:95–114.
[45] Janich P, Pascual G, Merlos-Suarez A, et al. The circadian molecular clock creates epidermal stem cell heterogeneity. Nature 2011;480:209–14.
[46] Puram RV, Kowalczyk MS, de Boer CG, et al. Core circadian clock genes regulate Leukemia stem cells in AML. Cell 2016;165:303–16.
[47] Ferrara N, Adamis AP. Ten years of anti-vascular endothelial growth factor therapy. Nat Rev Drug Discov 2016;15:385–403.
[48] Yesavage JA, Noda A, Hernandez B, et al. Circadian clock gene polymorphisms and sleep-wake disturbance in Alzheimer disease. Am J Geriatr Psychiatry 2011;19:635–43.
[49] Nievergelt CM, Kripke DF, Barrett TB, et al. Suggestive evidence for association of the circadian genes PERIOD3 and ARNTL with bipolar disorder. Am J Med Genet B Neuropsychiatr Genet 2006;141B:234–41.
[50] Chang YC, Chiu YF, Liu PH, et al. Genetic variation in the NOC gene is associated with body mass index in Chinese subjects. PLoS One 2013;8:e69622.

[51] Woldt E, Sebti Y, Solt LA, et al. Rev-erb-alpha modulates skeletal muscle oxidative capacity by regulating mitochondrial biogenesis and autophagy. Nat Med 2013;19:1039–46.
[52] Berthier A, Vinod M, Porez G, et al. Combinatorial regulation of hepatic cytoplasmic signaling and nuclear transcriptional events by the OGT/REV-ERBalpha complex. Proc Natl Acad Sci U S A 2018;115:E11033–42.
[53] Eichenfield DZ, Troutman TD, Link VM, et al. Tissue damage drives co-localization of NF-kappaB, Smad3, and Nrf2 to direct rev-erb sensitive wound repair in mouse macrophages. Elife 2016;5.
[54] Negoro H, Okinami T, Kanematsu A, et al. Role of rev-erbalpha domains for transactivation of the connexin43 promoter with Sp1. FEBS Lett 2013;587:98–103.
[55] Welch RD, Guo C, Sengupta M, et al. Rev-Erb co-regulates muscle regeneration via tethered interaction with the NF-Y cistrome. Mol Metab 2017;6:703–14.
[56] Gorbacheva VY, Kondratov RV, Zhang R, et al. Circadian sensitivity to the chemotherapeutic agent cyclophosphamide depends on the functional status of the CLOCK/BMAL1 transactivation complex. Proc Natl Acad Sci U S A 2005;102:3407–12.
[57] Korkmaz T, Aygenli F, Emisoglu H, et al. Opposite carcinogenic effects of circadian clock gene BMAL1. Sci Rep 2018;8:16023.
[58] Tang Q, Cheng B, Xie M, et al. Circadian clock gene Bmal1 inhibits tumorigenesis and increases paclitaxel sensitivity in tongue squamous cell carcinoma. Cancer Res 2017;77:532–44.
[59] Jiang W, Zhao S, Shen J, et al. The MiR-135b-BMAL1-YY1 loop disturbs pancreatic clockwork to promote tumourigenesis and chemoresistance. Cell Death Dis 2018;9:149.
[60] Zeng ZL, Luo HY, Yang J, et al. Overexpression of the circadian clock gene Bmal1 increases sensitivity to oxaliplatin in colorectal cancer. Clin Cancer Res 2014;20:1042–52.
[61] Kawamura G, Hattori M, Takamatsu K, et al. Cooperative interaction among BMAL1, HSF1, and p53 protects mammalian cells from UV stress. Commun Biol 2018;1:204.
[62] Lu H, Chu Q, Xie G, et al. Circadian gene expression predicts patient response to neoadjuvant chemoradiation therapy for rectal cancer. Int J Clin Exp Pathol 2015;8:10985–94.
[63] Iurisci I, Filipski E, Reinhardt J, et al. Improved tumor control through circadian clock induction by Seliciclib, a cyclin-dependent kinase inhibitor. Cancer Res 2006;66:10720–8.
[64] Debono M, Harrison RF, Chadarevian R, et al. Resetting the abnormal circadian cortisol rhythm in adrenal incidentaloma patients with mild autonomous cortisol secretion. J Clin Endocrinol Metab 2017;102:3461–9.
[65] Ballesta A, Dulong S, Abbara C, et al. A combined experimental and mathematical approach for molecular-based optimization of irinotecan circadian delivery. PLoS Comput Biol 2019;7:e1002143.
[66] Li XM, Mohammad-Djafari A, Dumitru M, et al. A circadian clock transcription model for the personalization of cancer chronotherapy. Cancer Res 2019;73:7176–88.
[67] Hirota T, Lee JW, St John PC, et al. Identification of small molecule activators of cryptochrome. Science 2012;337:1094–7.
[68] Sulli G, Rommel A, Wang X, et al. Pharmacological activation of REV-ERBs is lethal in cancer and oncogene-induced senescence. Nature 2018;553:351–5.
[69] Wang Y, Kojetin D, Burris TP. Anti-proliferative actions of a synthetic REV-ERBalpha/beta agonist in breast cancer cells. Biochem Pharmacol 2015;96:315–22.
[70] De Mei C, Ercolani L, Parodi C, et al. Dual inhibition of REV-ERBbeta and autophagy as a novel pharmacological approach to induce cytotoxicity in cancer cells. Oncogene 2015;34:2597–608.